Research article

Modeling HTLV-1 and HTLV-2 co-infection dynamics

E. A. Almohaimeed[1,*], **A. M. Elaiw**[2] **and A. D. Hobiny**[2]

[1] Department of Mathematics, College of Science, Qassim University, P. O. Box 53, Buraydah 51921, Saudi Arabia

[2] Department of Mathematics, Faculty of Science, King Abdulaziz University, P. O. Box 80203, Jeddah 21589, Saudi Arabia

* **Correspondence:** Email: E.Almohaimeed@qu.edu.sa.

Abstract: With the increasing prevalence of viral infections, the human T-cell leukemia virus (HTLV) is becoming a focal point of research. Of the four identified strains, HTLV-1 and HTLV-2 are particularly associated with various health issues. Both strains exhibit similar biological characteristics and transmission pathways, making them prevalent in specific high-risk populations, particularly among individuals who use injection drugs. HTLV-1 primarily targets the CD4$^+$ T cells, whereas HTLV-2 mainly affects the CD8$^+$ T cells. As far as we know, no mathematical model has been proposed to describe the within-host co-dynamics of HTLV-1 and HTLV-2. Therefore, this study presents a new mathematical framework to examine the within-host dynamics of HTLV-1 and HTLV-2 co-infection. Initially, the model's well-posedness is established by proving that the solutions remain both nonnegative and bounded over time. The equilibrium states and corresponding threshold conditions of the model are determined, and the criteria for the global asymptotic stability of each equilibrium are formulated. The global stability of the equilibria is analyzed using appropriate Lyapunov functions and LaSalle's invariance principle. These theoretical results are validated through numerical simulations. Additionally, sensitivity analysis of the basic reproduction numbers for HTLV-1 single infection (R_1) and HTLV-2 single infection (R_2) is performed to better understand the key parameters influencing co-infection dynamics. The study also explores the impact of CD8$^+$ T cell proliferation in the co-infection dynamics of HTLV-1 and HTLV-2, highlighting the importance of the CD8$^+$ T cell response in controlling the progression of HTLV-1. Furthermore, the impact of the viral infection rate on the co-infection dynamics of HTLV-1 and HTLV-2 is discussed. The results indicate that co-infection with HTLV-1 and HTLV-2 may increase the risk and severity of both viral infections.

Keywords: co-infection; global stability; HTLV-1; HTLV-2; Lyapunov function; sensitivity analysis
Mathematics Subject Classification: 34D20, 34D23, 37N25, 92B05

1. Introduction

Human T-cell leukemia virus (HTLV) is a family of retroviruses that predominantly target human T cells, a vital component of the immune system responsible for immune response regulation. HTLV is significant due to its link to various diseases and its capacity to persist in the human body over extended periods. Currently, four strains of this virus HTLV-1, HTLV-2, HTLV-3, and HTLV-4 are known to infect humans. Of these, only HTLV-1 and HTLV-2 have been associated with particular health issues [1]. These two strains share similar biological features and modes of transmission. HTLV-1 primarily targets $CD4^+$ T cells (also known as helper T cells) and is associated with two major diseases: adult T-cell leukemia (ATL) and a neurological disorder known as HTLV-1-associated myelopathy or tropical spastic paraparesis (HAM/TSP) [2]. On the other hand, HTLV-2 primarily infects $CD8^+$ T cells, commonly referred to as cytotoxic T lymphocytes (CTLs), which are essential for eliminating cells infected by viruses [2]. This strain has been connected to tropical spastic paraparesis as well as peripheral neuropathy [2]. People co-infected with HTLV-1 and HTLV-2 frequently face physical symptoms like chronic pain and weakness, along with social and psychological difficulties, such as depression and the stigma associated with carrying these viruses [3, 4]. The successful transmission of HTLV-1 and HTLV-2 to target cells necessitates direct interaction between cells (cell-to-cell) [5]. Both viruses rely on the envelope glycoproteins to mediate cell attachment and entry [5]. HTLV is spread through three primary pathways: from parent to child (e.g., during birth or breastfeeding), through parenteral exposure (such as infected blood transfusions, organ transplants, or sharing needles), and via sexual contact [5]. As of 2012, it was estimated that between five and ten million people globally were infected with HTLV-1. Regions with high prevalence included South America, the Caribbean, Southwest Japan, sub-Saharan Africa, the Middle East, and Australo Melanesia [6]. In contrast, HTLV-2 infections were significantly less common by 2015, with estimates ranging from 670,000 to 890,000 cases [7]. Most HTLV-2 cases were reported in the United States, particularly among Native American communities and intravenous drug users. Brazil, the country with the second-highest HTLV-2 prevalence, showed a similar distribution pattern. Infections with these viruses also aggravate other illnesses, such as tuberculosis and strongyloidiasis, which are widespread in endemic regions, adding to the challenges and expenses of their treatment [4, 8]. Although HTLV-1 and HTLV-2 co-infection is relatively uncommon, it has been identified in certain high-risk populations, especially among individuals who use injection drugs. The health consequences of these co-infections are not yet fully understood, highlighting the need for additional research to clarify their effects on disease progression and overall well-being. At present, no effective treatment exists for infections caused by HTLV-1 and HTLV-2, highlighting the importance of prevention and control measures to limit the dissemination of these viruses and reduce their impact on public health, especially in endemic regions [4].

The study of mathematical models offers a powerful and insightful approach to understanding the dynamics of viral infections within a host. This method enhances our comprehension of the mechanisms underlying diseases caused by different viruses. Recently, there has been an increased focus on mathematical models of HTLV-1 dynamics within a host, as they help to uncover the complex interactions between the virus, host cells, and the immune response. The model describing within-host HTLV-1 dynamics, incorporating the CTL-mediated immune response, is expressed as follows [9]:

$$\dot{U} = \underbrace{\alpha}_{\text{generation rate of healthy CD4}^+ \text{ T cells}} - \underbrace{\rho_U U}_{\text{mortality rate}} - \underbrace{\eta_{UH} UH}_{\text{infectivity rate}}, \tag{1.1}$$

$$\dot{H} = \underbrace{\eta_{UH} UH}_{\text{infectivity rate}} - \underbrace{\rho_H H}_{\text{mortality rate}} - \underbrace{\chi HC}_{\text{killing rate of HTLV-1-infected cells by CD8}^+ \text{ T cells}}, \tag{1.2}$$

$$\dot{C} = \underbrace{\sigma HC}_{\text{activation rate of CD8}^+ \text{ T cells}} - \underbrace{\rho_C C}_{\text{mortality rate}}. \tag{1.3}$$

Here,

$$U = U(t), \quad H = H(t) \quad \text{and} \quad C = C(t)$$

represent, respectively, the concentrations of healthy CD4$^+$ T cells, HTLV-1-infected CD4$^+$ T cells, and healthy CD8$^+$ T cells at time t. This mathematical model has been further expanded and refined by numerous researchers. Lim and Maini [10] developed a model to study HTLV-1 dynamics, factoring in CTL response and cell division. Pan et al. [11] created a model to describe HTLV dynamics, incorporating CTL response and time delays. Wang et al. [12] constructed a detailed HTLV-1 infection model that integrates nonlinear CTL responses (both lytic and nonlytic), a nonlinear incidence rate, distributed delays, and CTL dysfunction. Bera et al. [13] examined an HTLV-1 infection model that includes delayed CTL response. In another study, Wang et al. [14] investigated HTLV-1 dynamics using a model with two distinct delays: one for intracellular processes and another for CTL immune response. Papers [15–17] explored HTLV-1 dynamics with CTL response and cell division. Chen et al. [18] conducted a global dynamical analysis of an HTLV-1 infection model, incorporating logistic growth of CD4$^+$ T cells and nonlinear CTL response. Then the model was extended by taking into account delay CTL response [19] and environment noise [20]. The model proposed by [20] includes the impacts of reverse-transcriptase inhibitors and IL-2 immunotherapy, leading to the determination of an optimal therapeutic strategy. Wang and Ma [21] integrated CTL immunity and cell division into a diffusive model of HTLV infection. In contrast, research on HTLV-2 through mathematical modeling has been limited, with much less attention dedicated to its study.

Recent studies have focused on developing mathematical models to examine the co-infection dynamics of HTLV-1 with other viruses, such as HIV-1 (see, for instance, [22–26]) and SARS-CoV-2 [27]. A recent study by [28] developed and analyzed a co-infection model for HIV-1 and HTLV-2. As far as we can ascertain from a comprehensive review of the literature, no previous work has performed a dynamical analysis of HTLV-1 and HTLV-2 co-infection. Although various studies have explored HTLV-1 individually, we have not encountered any research that develops and examines a mathematical model specifically addressing the HTLV-1 and HTLV-2 co-infection dynamics.

This research focuses on formulating and examining a mathematical model that captures the dynamics of HTLV-1 and HTLV-2 co-infection within a host. The novelty of this study lies in the following key aspects:

B1. A novel co-infection model has been developed to describe the within-host interactions of HTLV-1 and HTLV-2, capturing their simultaneous presence in the host system.

B2. The model is structured based on the distinct cellular targets of each virus: HTLV-1 primarily infects CD4$^+$ T cells, whereas HTLV-2 predominantly targets CD8$^+$ T cells.

B3. A rigorous analysis of the model's solutions confirms their non-negativity and boundedness, ensuring both mathematical consistency and biological relevance.

B4. Four threshold parameters are established, which fully determine the conditions for the existence and stability of the model's equilibrium points.

B5. The global stability of each equilibrium is examined using the Lyapunov function approach.

B6. Theoretical results are substantiated through numerical simulations.

B7. A sensitivity analysis is conducted on the basic reproduction numbers for HTLV-1 (R_1) and HTLV-2 (R_2), assessing their dependence on key model parameters.

This methodology provides a comprehensive framework for examining the co-dynamics of HTLV variants and their impact on the host. HTLV-1 and HTLV-2 were chosen for this study due to their significant public health implications, their association with severe diseases, and their epidemiological relevance in HIV co-infection. Understanding their dynamics is crucial for enhancing disease control measures and developing effective intervention strategies. Moreover, the proposed model can be adapted to investigate the competitive transmission dynamics of different COVID-19 strains, such as Omicron and Delta.

The structure of this paper is as follows: Sections 2 and 3 introduce the formulation of the co-infection model, analyze the non-negativity and boundedness of its solutions, and derive the equilibrium points along with the threshold parameters. Section 4 explores the global stability of the equilibria. In Section 5, numerical simulations are conducted to validate the theoretical results. Finally, Section 6 provides a summary of the study's findings, discusses their implications, and suggests directions for future research.

2. Model formulation

This section provides a detailed description of the proposed model. The formulation of the model is based on the following assumptions:

A1. The model represents four populations: healthy CD4$^+$ T cells (U), HTLV-1-infected CD4$^+$ T cells (H), healthy CD8$^+$ T cells (C), and HTLV-2-infected CD8$^+$ T cells (M). The compartments U, H, C, and M have respective mortality rates of $\rho_U U$, $\rho_H H$, $\rho_C C$, and $\rho_M M$.

A2. Healthy CD4$^+$ T cells, which serve as the main targets for HTLV-1, are produced at a constant rate α. These cells can be infected by HTLV-1 through a cell-to-cell transmission mechanism at a rate of $\eta_{UH} UH$ [9] (see Eq (2.1)).

A3. HTLV-1-infected CD4$^+$ T cells are generated at a rate of $\eta_{UH} UH$. These infected cells are eliminated through immune-mediated destruction by CD8$^+$ T cells, at a rate represented by χHC [9] (see Eq (2.2)).

A4. Healthy CD8$^+$ T cells, the primary targets of HTLV-2, are produced at a constant rate γ (self-regulating immune response) and proliferate in response to the presence of HTLV-1-infected CD4$^+$ T cells at a rate of σHC (predator prey-like immune response) [9]. These cells can become infected through direct contact with HTLV-2-infected CD8$^+$ T cells via a cell-to-cell mechanism, at a rate described by $\eta_{CM} CM$ [5, 28] (see Eq (2.3)).

A5. HTLV-2-infected CD8$^+$ T cells are generated at a rate of $\eta_{CM}CM$ [28] (see Eq (2.4)).

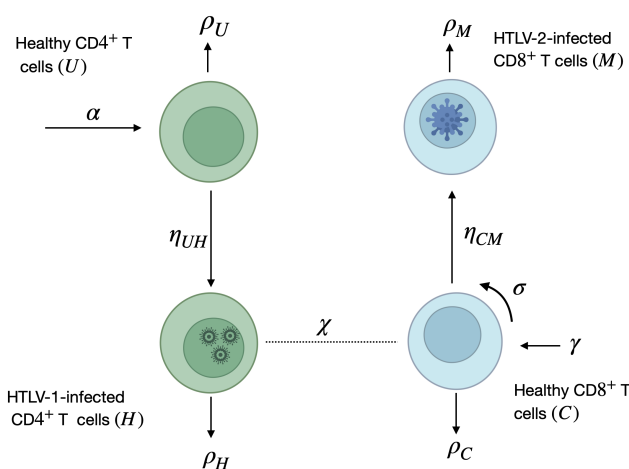Figure 1 illustrates the diagram that outlines the dynamics of HTLV-1 and HTLV-2 co-infection.

Figure 1. The diagram illustrates the co-dynamics model for HTLV-1 and HTLV-2.

According to assumptions A1–A5, the structure of the proposed models (2.1)–(2.4) is outlined as follows:

$$\dot{U} = \alpha - \rho_U U - \eta_{UH}UH, \tag{2.1}$$

$$\dot{H} = \eta_{UH}UH - \rho_H H - \chi HC, \tag{2.2}$$

$$\dot{C} = \gamma + \sigma HC - \rho_C C - \eta_{CM}CM, \tag{2.3}$$

$$\dot{M} = \eta_{CM}CM - \rho_M M. \tag{2.4}$$

The descriptions and values of the variables and parameters are shown in Table 1.

Table 1. Model parameters.

Symbol	Description	Value	Source
U	Concentration of healthy CD4$^+$ T cells	cells μL^{-1}	–
H	Concentration of HTLV-1 infected CD4$^+$ T cells	cells μL^{-1}	–
C	Concentration of healthy CD8$^+$ T cells	cells μL^{-1}	–
M	Concentration of HTLV-2-infected CD8$^+$ T cells	cells μL^{-1}	–
α	Production rate of healthy CD4$^+$ T cells	10 cells μL^{-1} day^{-1}	[15, 29]
ρ_U	Mortality rate of healthy CD4$^+$ T cells	0.01 day^{-1}	[30, 31]
η_{UH}	Incidence rate due to CTC contact between HTLV-1-infected and healthy CD4$^+$ T cells	varied	–
ρ_H	Mortality rate of HTLV-1 infected CD4$^+$ T cells	0.05 day^{-1}	[11, 12, 14]
χ	killing rate of HTLV-1-infected CD4$^+$ T cells due to CD8$^+$ T cells	0.02 cells $^{-1}$ μL day^{-1}	[11, 12, 14, 32]
γ	Generation rate of healthy CD8$^+$ T cells	20 cells μL^{-1} day^{-1}	[33]
σ	Activation rate of healthy CD8$^+$ T cells	0.2 cells^{-1} μL day^{-1}	[34]
ρ_C	Mortality rate of healthy CD8$^+$ T cells	0.06 day^{-1}	[33]
η_{CM}	Incidence rate due to CTC contact between HTLV-2-infected and healthy CD8$^+$ T cells	varied	–
ρ_M	Mortality rate of HTLV-2-infected CD8$^+$ T cells	0.3 day^{-1}	Assumed

Remark 1. We mention that we have used bilinear incidence rate for the infection rate. This form is commonly used in mathematical virology due to its simplicity and analytical tractability while capturing the fundamental interaction between target cells and viruses or infected cells (see, e.g., [9–11, 17]). Specifically, the terms $\eta_{UH}UH$ and $\eta_{CM}CM$ represent the infection rates proportional to the product of interacting populations, aligning with the standard mass-action principle. Some modifed versions for the infection rate have been included in the HTLV-1 models, such as:

- Saturated incidence: $\frac{\eta_{UH}UH}{1+mH}$, where $m \geq 0$. This incidence form can be suitable when the concentration of infected T cells becomes significantly high [35].

- Holling type-I: $\frac{\eta_{UH}UH}{1+nU}$ [16].

- Beddington-DeAngelis incidence: $\frac{\eta_{UH}UH}{1+nU+mH}$, where $n, m \geq 0$ [36].

- Crowley Martin incidence: $\frac{\eta_{UH}UH}{(1+nU)(1+mH)}$ [12].

- Nonlinear incidence: $\eta_{UH}U^pH^q$, where p and q are positive constants [21]. Another form, presented in [37, 38] as $\Psi(H)U$, where Ψ is a nonlinear function. In [12], the bilinear incidence $\eta_{UH}UH$ was adjusted to $\frac{\eta_{UH}UH}{1+q_0C}$ to incorporate the impact of the non-lytic CTL (NL-CTL) response, which suppresses viral replication through soluble mediators. Here, q_0 represents the effectiveness of the NL-CTL response.

- Standard incidence: $\frac{\eta_{UH}UH}{U+H}$, [39]. This form has been generalized in [40] as $\frac{\eta_{UH}UH}{(U+H)^\varepsilon}$, where $0 \leq \varepsilon \leq 1$.

- General incidence: $\Psi(U, H)H$, where $\Psi(U, H)$ is a general function that is the average number of healthy CD4$^+$ T cells that are infected by unit HTLV-1-infected CD4$^+$ T cells per unit time [21]. In [41], a general incidence in the form $\Psi(U, H)$ is considered.

Due to the limited experimental data specifically quantifying HTLV-1 and HTLV-2 co-infection transmission rates, we adopted this bilinear incidence as a reasonable first approximation.

3. Preliminaries

This section analyzes the essential qualitative characteristics of the systems (2.1)–(2.4), including the solutions' nonnegativity and boundedness of solutions. Moreover, each equilibrium is identified together with its corresponding threshold number.

3.1. Non-negativity and boundedness of solutions

In this subsection, we establish the well-posedness of the models (2.1)–(2.4) by demonstrating that the solutions remain nonnegative and bounded over time.

Lemma 1. *Solutions of the systemS (2.1)–(2.4) are nonnegative and bounded.*

Proof. We have

$$\dot{U}\mid_{U=0} = \alpha > 0, \quad \dot{H}\mid_{H=0} = 0, \quad \dot{C}\mid_{C=0} = \gamma > 0, \quad \dot{M}\mid_{M=0} = 0.$$

Hence, in conformity with [42, Proposition B.7]

$$(U, H, C, M)(t) \in \mathbb{R}^4_{\geq 0}$$

for any $t \geq 0$, when

$$(U, H, C, M)(0) \in \mathbb{R}^4_{\geq 0}.$$

To illustrate the boundedness of the solutions. Let's establish the definition of $\psi(t)$ as:

$$\psi = U + H + \frac{\chi}{\sigma} [C + M].$$

Next, we obtain

$$\dot{\psi} = \dot{U} + \dot{H} + \frac{\chi}{\sigma} \left[\dot{C} + \dot{M} \right]$$

$$= \alpha - \rho_U U - \eta_{UH} UH + \eta_{UH} UH - \rho_H H - \chi HC + \frac{\chi}{\sigma} [\gamma + \sigma HC - \rho_C C - \eta_{CM} CM + \eta_{CM} CM - \rho_M M]$$

$$= \alpha + \frac{\chi\gamma}{\sigma} - \rho_U U - \rho_H H - \frac{\chi\rho_C}{\sigma} C - \frac{\chi\rho_M}{\sigma} M$$

$$\leq \alpha + \frac{\chi\gamma}{\sigma} - \varrho \left[U + H + \frac{\chi}{\sigma} (C + M) \right]$$

$$= \alpha + \frac{\chi\gamma}{\sigma} - \varrho\psi,$$

where

$$\varrho = \min\{\rho_U, \rho_H, \rho_C, \rho_M\}.$$

Thus,

$$\psi(t) \leq \frac{\alpha}{\varrho} + \frac{\chi\gamma}{\sigma\varrho} = \tau_1$$

if

$$\psi(0) \leq \tau_1.$$

Consequently

$$0 \leq U(t), \quad H(t) \leq \tau_1, \quad 0 \leq C(t), \quad M(t) \leq \tau_2$$

if

$$U(0) + H(0) + \frac{\chi}{\sigma} [C(0) + M(0)] \leq \tau_1,$$

where

$$\tau_2 = \frac{\sigma}{\chi} \tau_1.$$

This completes the proof. □

3.2. Equilibria and thresholds

Define

$$U_0 = \frac{\alpha}{\rho_U}$$

and

$$C_0 = \frac{\gamma}{\rho_C},$$

and introduce the following four indices, which will serve as threshold parameters, denoted by

$$R_i, i = 1, 2, 3, 4$$

and given by

$$R_1 = \frac{\alpha \eta_{UH} \rho_C}{\rho_U (\rho_H \rho_C + \chi \gamma)}, \quad R_2 = \frac{\gamma \eta_{CM}}{\rho_M \rho_C}, \quad R_3 = \frac{\eta_{UH} \eta_{CM} \alpha}{\rho_U (\eta_{CM} \rho_H + \chi \rho_M)},$$

$$R_4 = \frac{\eta_{UH} \eta_{CM}}{\eta_{UH} \rho_C + \rho_U \sigma} \left(\frac{\gamma}{\rho_M} + \frac{\sigma \alpha}{\eta_{CM} \rho_H + \chi \rho_M} \right). \tag{3.1}$$

It is crucial to highlight that R_1 indicates the basic reproduction number for HTLV-1 single infection and represents the number of new CD4$^+$ T cells infected with HTLV-1 that are generated from a single HTLV-1-infected CD4$^+$ T cell during the early phase of HTLV-1 single infection. The parameter R_2 stands for the basic reproduction number for HTLV-2 single infection and represents the quantity of newly infected CD8$^+$ T cells carrying HTLV-2 that originate from one HTLV-2-infected CD8$^+$ T cell in the initial phases of HTLV-2 single infection. The threshold values R_3 and R_4 serve as indicators of the likelihood of co-infection with HTLV-1 and HTLV-2.

Lemma 2. *For the models (2.1)–(2.4), four equilibrium points (EPs) exist, such that*

(I) *Disease-free equilibrium, EP_0, is always presented, where*

$$EP_0 = (U_0, 0, C_0, 0).$$

(II) *If $R_1 > 1$, an equilibrium for HTLV-1 single infection,*

$$EP_1 = (U_1, H_1, C_1, 0)$$

will emerge in addition to EP_0.

(III) *If $R_2 > 1$, an equilibrium for HTLV-2 single infection,*

$$EP_2 = (U_2, 0, C_2, M_2)$$

will emerge in addition to EP_0.

(IV) *If $R_3 > 1$ and $R_4 > 1$, an equilibrium HTLV-1/HTLV-2 co-infection,*

$$EP_3 = (U_3, H_3, C_3, M_3)$$

will emerge in addition to EP_0.

Proof. The EPs of models (2.1)–(2.4) satisfy the following:

$$\begin{cases} 0 = \alpha - \rho_U U - \eta_{UH} UH, \\ 0 = \eta_{UH} UH - \rho_H H - \chi HC, \\ 0 = \gamma + \sigma HC - \rho_C C - \eta_{CM} CM, \\ 0 = \eta_{CM} CM - \rho_M M. \end{cases} \tag{3.2}$$

Solving the algebraic system (3.2), we obtain four equilibrium points as follows:

(1) Disease-free equilibrium,
$$EP_0 = (U_0, 0, C_0, , 0).$$

(2) HTLV-1 single infection equilibrium,
$$EP_1 = (U_1, H_1, C_1, 0),$$

where
$$U_1 = \frac{\rho_H + \chi C_1}{\eta_{UH}}, \quad C_1 = \frac{\gamma}{\rho_C - \sigma H_1}$$

and H_1 fulfills the following:
$$\frac{a_1 H_1^2 + a_2 H_1 + a_3}{\rho_C - \sigma H_1} = 0,$$

where
$$a_1 = \rho_H \eta_{UH} \sigma,$$
$$a_2 = \rho_U \rho_H \sigma - \sigma \alpha \eta_{UH} - \rho_H \eta_{UH} \rho_C - \chi \gamma \eta_{UH},$$
$$a_3 = \alpha \eta_{UH} \rho_C - \rho_U (\rho_H \rho_C + \chi \gamma).$$

Let us define a function $\mathcal{D}(H)$ as follows:
$$\mathcal{D}(H) = \frac{a_1 H^2 + a_2 H + a_3}{\rho_C - \sigma H} = 0, \, H \in \left[0, \frac{\rho_C}{\sigma}\right).$$

Note that, $\mathcal{D}$ is continuous on $\left[0, \frac{\rho_C}{\sigma}\right)$. We have
$$\mathcal{D}(0) = \frac{\alpha \eta_{UH} \rho_C - \rho_U (\rho_H \rho_C + \chi \gamma)}{\rho_C} = \frac{\rho_U (\rho_H \rho_C + \chi \gamma)}{\rho_C} (R_1 - 1).$$

The presence of an HTLV-1 single infection is determined by evaluating the parameter R_1. Since
$$\mathcal{D}(0) > 0$$

if $R_1 > 1$ in addition to
$$\lim_{H \to \left(\frac{\rho_C}{\sigma}\right)^-} \mathcal{D}(H) = -\infty,$$

there exists H_1 such that
$$0 < H_1 < \frac{\rho_C}{\sigma}$$

and satisfies
$$\mathcal{D}(H_1) = 0.$$

Consequently, we obtain $U_1 > 0$, and $C_1 > 0$.

(3) HTLV-2 single infection equilibrium,
$$EP_2 = (U_2, 0, C_2, M_2),$$

where
$$U_2 = \frac{\alpha}{\rho_U} = U_0, C_2 = \frac{\rho_M}{\eta_{CM}} = \frac{C_0}{R_2}, M_2 = \frac{\rho_C}{\eta_{CM}} (R_2 - 1).$$

The persistence of an HTLV-2 single infection can be ascertained by assessing the parameter R_2.

(4) HTLV-1/HTLV-2 co-infection equilibrium,

$$EP_3 = (U_3, H_3, C_3, M_3),$$

where

$$U_3 = \frac{\eta_{CM}\rho_H + \chi\rho_M}{\eta_{UH}\eta_{CM}}, \quad H_3 = \frac{\rho_U}{\eta_{UH}}(R_3 - 1), \quad C_3 = \frac{\rho_M}{\eta_{CM}}, \quad M_3 = \frac{\eta_{UH}\rho_C + \rho_U\sigma}{\eta_{UH}\eta_{CM}}(R_4 - 1).$$

This completes the proof. □

4. Global stability

This section aims to examine the global asymptotic stability of all EPs in the models (2.1)–(2.4) using the Lyapunov approach, as proposed in the work conducted by [43]. We define a function

$$\mathcal{F}(x) = x - (1 + \ln x).$$

Moreover, the arithmetic mean-geometric mean inequality is utilized to establish the proofs of Theorems 1–4 as:

$$\frac{1}{m}\sum_{k=1}^{m} S_k \geq \left(\prod_{k=1}^{m} S_k\right)^{\frac{1}{m}}, \quad S_k \geq 0, \quad k = 1, 2, ..., m. \tag{4.1}$$

Let $\mathcal{L}_k$ be the candidate Lyapunov function and define $\mathcal{H}'_k$ as the largest invariant set of

$$\mathcal{H}_k = \left\{(U, H, C, M) : \frac{d\mathcal{L}_k}{dt} = 0\right\}, \quad \text{where } k = 0, 1, 2, 3.$$

Theorem 1. *The disease-free equilibrium EP_0 is globally asymptotically stable (GAS) if $R_1 \leq 1$ and $R_2 \leq 1$; otherwise, it is unstable.*

Proof. To verify (i), we define $\mathcal{L}_0(U, H, C, M)$ as:

$$\mathcal{L}_0 = U_0\mathcal{F}\left(\frac{U}{U_0}\right) + H + \frac{\chi}{\sigma}C_0\mathcal{F}\left(\frac{C}{C_0}\right) + \frac{\chi}{\sigma}M.$$

Obviously,

$$\mathcal{L}_0(U, H, C, M) > 0$$

for any

$$U, H, C, M > 0$$

and

$$\mathcal{L}_0(U_0, 0, C_0, 0) = 0.$$

The derivative of $\mathcal{L}_0$ along the solutions of systems (2.1)–(2.4) can be computed as:

$$\frac{d\mathcal{L}_0}{dt} = \left(1 - \frac{U_0}{U}\right)\dot{U} + \dot{H} + \frac{\chi}{\sigma}\left(1 - \frac{C_0}{C}\right)\dot{C} + \frac{\chi}{\sigma}\dot{M}.$$

By substituting the equations stated in models (2.1)–(2.4), we derive

$$\frac{d\mathcal{L}_0}{dt} = \left(1 - \frac{U_0}{U}\right)(\alpha - \rho_U U - \eta_{UH}UH) + (\eta_{UH}UH - \rho_H H - \chi HC)$$
$$+ \frac{\chi}{\sigma}\left(1 - \frac{C_0}{C}\right)(\gamma + \sigma HC - \rho_C C - \eta_{CM}CM) + \frac{\chi}{\sigma}(\eta_{CM}CM - \rho_M M).$$

By gathering the terms and substituting α with $\rho_U U_0$ and γ with $\rho_C C_0$, we derive the following expression:

$$\frac{d\mathcal{L}_0}{dt} = \frac{-\rho_U}{U}(U - U_0)^2 - \frac{\chi}{\sigma}\frac{\rho_C}{C}(C - C_0)^2 + \eta_{UH}U_0 H - \rho_H H - \chi C_0 H + \frac{\chi\eta_{CM}}{\sigma}C_0 M - \frac{\chi\rho_M}{\sigma}M$$
$$= \frac{-\rho_U}{U}(U - U_0)^2 - \frac{\chi}{\sigma}\frac{\rho_C}{C}(C - C_0)^2 + (\eta_{UH}U_0 - \rho_H - \chi C_0)H + \frac{\chi}{\sigma}(\eta_{CM}C_0 - \rho_M)M.$$

Then,

$$\frac{d\mathcal{L}_0}{dt} = \frac{-\rho_U}{U}(U - U_0)^2 - \frac{\chi}{\sigma}\frac{\rho_C}{C}(C - C_0)^2$$
$$+ \frac{\rho_H \rho_C + \chi\gamma}{\rho_C}\left(\frac{\alpha\eta_{UH}\rho_C}{\rho_U(\rho_H\rho_C + \chi\gamma)} - 1\right)H + \frac{\chi\rho_M}{\sigma}\left(\frac{\gamma\eta_{CM}}{\rho_M\rho_C} - 1\right)M.$$

Ultimately, we obtain

$$\frac{d\mathcal{L}_0}{dt} = \frac{-\rho_U}{U}(U - U_0)^2 - \frac{\chi}{\sigma}\frac{\rho_C}{C}(C - C_0)^2 + \frac{\rho_H\rho_C + \chi\gamma}{\rho_C}(R_1 - 1)H + \frac{\chi\rho_M}{\sigma}(R_2 - 1)M.$$

Thus,

$$\frac{d\mathcal{L}_0}{dt} \leq 0$$

satisfies if $R_1 \leq 1$ and $R_2 \leq 1$. Moreover,

$$\frac{d\mathcal{L}_0}{dt} = 0,$$

when

$$U = U_0, \quad C = C_0, \quad (R_1 - 1)H = 0 \quad \text{and} \quad (R_2 - 1)M = 0.$$

The solutions of the system approach $\mathcal{H}_0'$ [44]. Every element in $\mathcal{H}_0'$ satisfies $U = U_0$, $C = C_0$,

$$(R_1 - 1)H = 0 \quad \text{and} \quad (R_2 - 1)M = 0. \tag{4.2}$$

As a result, four cases arise:

(I) $R_1 = 1$ and $R_2 = 1$. Then from Eq (2.1) we obtain

$$\dot{U} = \alpha - \rho_U U_0 - \eta_{UH}U_0 H = 0 \implies H(t) = 0 \quad \text{for any } t. \tag{4.3}$$

From Eq (2.3) we have

$$\dot{C} = \gamma - \rho_C C_0 - \eta_{CM}C_0 M = 0 \implies M(t) = 0 \quad \text{for any } t. \tag{4.4}$$

Hence,

$$\mathcal{H}_0' = \{EP_0\}.$$

(II) $R_1 < 1$ and $R_2 < 1$. Then, Eq (4.2) implies that $H = M = 0$ and, hence,

$$\mathcal{H}_0' = \{EP_0\}.$$

(III) $R_1 = 1$ and $R_2 < 1$. Then, Eq (4.2) suggests $M = 0$ and Eq (4.3) gives $H = 0$. Thus,

$$\mathcal{H}_0' = \{EP_0\}.$$

(IV) $R_1 < 1$ and $R_2 = 1$. Eq (4.2) gives $H = 0$ while Eq (4.4) implies $M = 0$. Consequently,

$$\mathcal{H}_0' = \{EP_0\}.$$

By LaSalle's invariance principle (LP) [45], EP_0 is GAS.

Now, let us establish the instability of EP_0 if $R_1 > 1$ and/or $R_2 > 1$. First of all, we construct the Jacobian matrix

$$\mathcal{J} = \mathcal{J}(U, H, C, M)$$

of models (2.1)–(2.4) as:

$$\mathcal{J} = \begin{pmatrix} -\rho_U - \eta_{UH}H & -\eta_{UH}U & 0 & 0 \\ \eta_{UH}H & \eta_{UH}U - \rho_H - \chi C & -\chi H & 0 \\ 0 & \sigma C & \sigma H - \rho_C - \eta_{CM}M & -\eta_{CM}C \\ 0 & 0 & \eta_{CM}M & \eta_{CM}C - \rho_M \end{pmatrix}. \qquad (4.5)$$

Next, we calculate the characteristic equation at the equilibrium point EP_0 as:

$$\det(\mathcal{J} - \Lambda I) = (\Lambda + \rho_U)(\Lambda + \rho_C)(k_1\Lambda + k_0)(f_1\Lambda + f_0) = 0, \qquad (4.6)$$

where Λ represents the eigenvalue, I represents the identity matrix, and

$$k_1 = \rho_U\rho_C,$$
$$k_0 = \rho_U(\rho_H\rho_C + \chi\gamma) - \alpha\eta_{UH}\rho_C = \rho_U(\rho_H\rho_C + \chi\gamma)(1 - R_1),$$
$$f_1 = \rho_C,$$
$$f_0 = \rho_M\rho_C - \gamma\eta_{CM} = \rho_M\rho_C(1 - R_2).$$

Then matrix J has the following eigenvalues:

$$\Lambda_1 = -\rho_U, \ \Lambda_2 = -\rho_C,$$
$$\Lambda_3 = -k_0/k_1 = -\frac{(\rho_H\rho_C + \chi\gamma)}{\rho_C}(1 - R_1),$$
$$\Lambda_4 = -f_0/f_1 = -\rho_M(1 - R_2).$$

Clearly, $\Lambda_3 > 0$ and $\Lambda_4 > 0$, when $R_1 > 1$ and $R_2 > 1$. It follows that if either $R_1 > 1$, $R_2 > 1$, or both, then EP_0 is unstable.

This completes the proof. $\qquad\qquad\square$

Theorem 2. *HTLV-1 single infection equilibrium EP_1 is GAS if $R_1 > 1$ and $R_4 \leq 1$.*

Proof. Construct $\mathcal{L}_1(U, H, C, M)$ as:

$$\mathcal{L}_1 = U_1 \mathcal{F}\left(\frac{U}{U_1}\right) + H_1 \mathcal{F}\left(\frac{H}{H_1}\right) + \frac{\chi}{\sigma} C_1 \mathcal{F}\left(\frac{C}{C_1}\right) + \frac{\chi}{\sigma} M.$$

Clearly,

$$\mathcal{L}_1(U, H, C, M) > 0$$

for any

$$U, H, C, M > 0$$

and

$$\mathcal{L}_1(U_1, H_1, C_1, 0) = 0.$$

Calculating $\frac{d\mathcal{L}_1}{dt}$ as:

$$\frac{d\mathcal{L}_1}{dt} = \left(1 - \frac{U_1}{U}\right)(\alpha - \rho_U U - \eta_{UH} UH) + \left(1 - \frac{H_1}{H}\right)(\eta_{UH} UH - \rho_H H - \chi HC)$$

$$+ \frac{\chi}{\sigma}\left(1 - \frac{C_1}{C}\right)(\gamma + \sigma HC - \rho_C C - \eta_{CM} CM) + \frac{\chi}{\sigma}(\eta_{CM} CM - \rho_M M).$$

Collecting terms results to

$$\frac{d\mathcal{L}_1}{dt} = \left(1 - \frac{U_1}{U}\right)(\alpha - \rho_U U) + \eta_{UH} U_1 H - \eta_{UH} H_1 U - \rho_H H + \rho_H H_1$$

$$+ \chi H_1 C + \frac{\chi}{\sigma}\left(1 - \frac{C_1}{C}\right)(\gamma - \rho_C C) - \chi C_1 H + \frac{\chi \eta_{CM}}{\sigma} C_1 M - \frac{\chi \rho_M}{\sigma} M.$$

By using the subsequent equilibrium conditions

$$\begin{cases} \alpha = \rho_U U_1 + \eta_{UH} U_1 H_1, \\ \eta_{UH} U_1 H_1 = \rho_H H_1 + \chi H_1 C_1, \\ \gamma = \rho_C C_1 - \sigma H_1 C_1, \end{cases}$$

we obtain

$$\frac{d\mathcal{L}_1}{dt} = \frac{-\rho_U}{U}(U - U_1)^2 - \frac{\chi}{\sigma}\frac{\rho_C}{C}(C - C_1)^2 + \left(1 - \frac{U_1}{U}\right)\eta_{UH} U_1 H_1 - \chi\left(1 - \frac{C_1}{C}\right) H_1 C_1$$

$$+ (\eta_{UH} U_1 H_1 - \rho_H H_1 - \chi C_1 H_1)\frac{H}{H_1} + \frac{\chi \eta_{CM}}{\sigma}\left(C_1 - \frac{\rho_M}{\eta_{CM}}\right) M - \eta_{UH} U_1 H_1 \frac{U}{U_1}$$

$$+ \rho_H H_1 + \chi H_1 C_1 \frac{C}{C_1} + \chi H_1 C_1 - \chi H_1 C_1.$$

It follows that

$$\frac{d\mathcal{L}_1}{dt} = \frac{-\rho_U}{U}(U - U_1)^2 - \frac{\chi}{\sigma}\frac{\rho_C}{C}(C - C_1)^2 + \left(2 - \frac{U_1}{U} - \frac{U}{U_1}\right)\eta_{UH} U_1 H_1$$

$$- \chi\left(2 - \frac{C_1}{C} - \frac{C}{C_1}\right) H_1 C_1 + \frac{\chi \eta_{CM}}{\sigma}\left(C_1 - \frac{\rho_M}{\eta_{CM}}\right) M$$

$$= \frac{-\alpha}{UU_1}(U - U_1)^2 - \frac{\chi}{\sigma}\frac{\gamma}{CC_1}(C - C_1)^2 + \frac{\chi\eta_{CM}}{\sigma}(C_1 - C_3)M.$$

We will now demonstrate that if

$$R_4 \leq 1 \Leftrightarrow C_1 \leq C_3$$

as:

$$C_1 \leq C_3 \Leftrightarrow \frac{\alpha\eta_{UH}\sigma + \gamma\eta_{UH}\chi - \eta_{UH}\rho_C\rho_H - \rho_U\sigma\rho_H + \sqrt{4\gamma\eta_{UH}(\eta_{UH}\rho_C + \rho_U\sigma)\chi\rho_H + (\alpha\eta_{UH}\sigma + \gamma\eta_{UH}\chi - (\eta_{UH}\rho_C + \rho_U\sigma)\rho_H)^2}}{2(\eta_{UH}\rho_C + \rho_U\sigma)\chi}$$

$$\leq \frac{\rho_M}{\eta_{CM}}$$

$$\Leftrightarrow \alpha\eta_{UH}\sigma + \gamma\eta_{UH}\chi - \eta_{UH}\rho_C\rho_H - \rho_U\sigma\rho_H + \sqrt{4\gamma\eta_{UH}(\eta_{UH}\rho_C + \rho_U\sigma)\chi\rho_H + (\alpha\eta_{UH}\sigma + \gamma\eta_{UH}\chi - (\eta_{UH}\rho_C + \rho_U\sigma)\rho_H)^2}$$

$$\leq \frac{2(\eta_{UH}\rho_C + \rho_U\sigma)\chi\rho_M}{\eta_{CM}}$$

$$\Leftrightarrow \sqrt{4\gamma\eta_{UH}(\eta_{UH}\rho_C + \rho_U\sigma)\chi\rho_H + (\alpha\eta_{UH}\sigma + \gamma\eta_{UH}\chi - (\eta_{UH}\rho_C + \rho_U\sigma)\rho_H)^2}$$

$$\leq \frac{2(\eta_{UH}\rho_C + \rho_U\sigma)\chi\rho_M}{\eta_{CM}} - (\alpha\eta_{UH}\sigma + \gamma\eta_{UH}\chi - \eta_{UH}\rho_C\rho_H - \rho_U\sigma\rho_H)$$

$$\Leftrightarrow 4\gamma\eta_{UH}(\eta_{UH}\rho_C + \rho_U\sigma)\chi\rho_H + (\alpha\eta_{UH}\sigma + \gamma\eta_{UH}\chi - (\eta_{UH}\rho_C + \rho_U\sigma)\rho_H)^2$$

$$\leq \left(\frac{2(\eta_{UH}\rho_C + \rho_U\sigma)\chi\rho_M}{\eta_{CM}} - (\alpha\eta_{UH}\sigma + \gamma\eta_{UH}\chi - \eta_{UH}\rho_C\rho_H - \rho_U\sigma\rho_H)\right)^2$$

$$\Leftrightarrow \alpha\eta_{UH}\eta_{CM}\sigma\rho_M + \gamma\eta_{UH}\eta_{CM}(\eta_{CM}\rho_H + \chi\rho_M)$$

$$\leq \rho_M(\eta_{UH}\rho_C + \rho_U\sigma)(\eta_{CM}\rho_H + \chi\rho_M)$$

$$\Leftrightarrow \frac{\alpha\eta_{UH}\eta_{CM}\sigma\rho_M + \gamma\eta_{UH}\eta_{CM}(\eta_{CM}\rho_H + \chi\rho_M)}{\rho_M(\eta_{UH}\rho_C + \rho_U\sigma)(\eta_{CM}\rho_H + \chi\rho_M)} \leq 1$$

$$\Leftrightarrow \frac{\eta_{UH}\eta_{CM}}{\eta_{UH}\rho_C + \rho_U\sigma}\left(\frac{\gamma}{\rho_M} + \frac{\sigma\alpha}{\eta_{CM}\rho_H + \chi\rho_M}\right) \leq 1$$

$$\Leftrightarrow R_4 \leq 1.$$

Thus, by applying inequality (4.1), it follows that

$$\frac{d\mathcal{L}_1}{dt} \leq 0$$

for all

$$U, H, C, M > 0.$$

In addition,

$$\frac{d\mathcal{L}_1}{dt} = 0$$

if

$$U = U_1, \quad C = C_1 \quad \text{and} \quad (C_1 - C_3)M = 0.$$

The solutions of models (2.1)–(2.4) approach $\mathcal{H}_1'$, where

$$U = U_1, \quad C = C_1$$

and

$$(C_1 - C_3)M = 0. \tag{4.7}$$

As a result, two cases arise:

(I) $C_1 = C_3$, then from Eq (2.1)

$$\dot{U} = \alpha - \rho_U U_1 - \eta_{UH} U_1 H = 0 \implies H(t) = H_1 \quad \text{for any } t. \tag{4.8}$$

From Eq (2.3), we have

$$\dot{C} = \gamma + \sigma H_1 C_1 - \rho_C C_1 - \eta_{CM} C_1 M = 0 \implies M(t) = 0 \quad \text{for any } t. \tag{4.9}$$

Then,

$$\mathcal{H}_1' = \{EP_1\}.$$

(II) $C_1 < C_3$, then Eq (4.7) implies that $M = 0$ and Eq (4.8) gives $H = H_1$. Hence,

$$\mathcal{H}_1' = \{EP_1\}.$$

Thus, by LP, EP_1 is GAS. $\qquad\qquad\qquad\qquad\qquad\qquad\qquad\qquad\qquad\qquad\qquad\qquad\quad\square$

Theorem 3. *HTLV-2 single infection equilibrium, EP_2 is GAS if $R_2 > 1$ and $R_3 \leq 1$, and if $R_3 > 1$, then EP_2 is unstable.*

Proof. Define $\mathcal{L}_2(U, H, C, M)$ as:

$$\mathcal{L}_2 = U_2 \mathcal{F}\left(\frac{U}{U_2}\right) + H + \frac{\chi}{\sigma} C_2 \mathcal{F}\left(\frac{C}{C_2}\right) + \frac{\chi}{\sigma} M_2 \mathcal{F}\left(\frac{M}{M_2}\right).$$

Evidently,

$$\mathcal{L}_2(U, H, C, M) > 0$$

for any

$$U, H, C, M > 0$$

and

$$\mathcal{L}_2(U_2, 0, C_2, M_2) = 0.$$

Calculating $\frac{d\mathcal{L}_2}{dt}$ as:

$$\frac{d\mathcal{L}_2}{dt} = \left(1 - \frac{U_2}{U}\right)(\alpha - \rho_U U - \eta_{UH} UH) + (\eta_{UH} UH - \rho_H H - \chi HC)$$
$$+ \frac{\chi}{\sigma}\left(1 - \frac{C_2}{C}\right)(\gamma + \sigma HC - \rho_C C - \eta_{CM} CM) + \frac{\chi}{\sigma}\left(1 - \frac{M_2}{M}\right)(\eta_{CM} CM - \rho_M M).$$

Collecting the above terms leads to

$$\frac{d\mathcal{L}_2}{dt} = \left(1 - \frac{U_2}{U}\right)(\alpha - \rho_U U) + \eta_{UH} U_2 H - \rho_H H + \frac{\chi}{\sigma}\left(1 - \frac{C_2}{C}\right)(\gamma - \rho_C C)$$
$$- \chi C_2 H + \frac{\chi \eta_{CM}}{\sigma} C_2 M - \frac{\chi \eta_{CM}}{\sigma} M_2 C - \frac{\chi \rho_M}{\sigma} M + \frac{\chi \rho_M}{\sigma} M_2.$$

Utilizing the equilibrium conditions

$$\alpha = \rho_U U_2, \quad \gamma = \rho_C C_2 + \eta_{CM} C_2 M_2, \quad C_2 = \frac{\rho_M}{\eta_{CM}}.$$

We obtain

$$
\begin{aligned}
\frac{d\mathcal{L}_2}{dt} &= \frac{-\rho_U}{U}(U - U_2)^2 - \frac{\chi}{\sigma}\frac{\rho_C}{C}(C - C_2)^2 + \frac{\chi}{\sigma}\left(1 - \frac{C_2}{C}\right)\eta_{CM}C_2 M_2 + (\eta_{UH}U_2 - \rho_H - \chi C_2)H \\
&\quad - \frac{\chi}{\sigma}\eta_{CM}M_2 C_2 \frac{C}{C_2} + \frac{\chi}{\sigma}\eta_{CM}C_2 M_2 \\
&= \frac{-\rho_U}{U}(U - U_2)^2 - \frac{\chi}{\sigma}\frac{\rho_C}{C}(C - C_2)^2 + \frac{\chi}{\sigma}\left(2 - \frac{C_2}{C} - \frac{C}{C_2}\right)\eta_{CM}C_2 M_2 \\
&\quad + \frac{\eta_{CM}\rho_H + \chi\rho_M}{\eta_{CM}}\left(\frac{\eta_{UH}\eta_{CM}\alpha}{\rho_U(\eta_{CM}\rho_H + \chi\rho_M)} - 1\right)H \\
&= \frac{-\rho_U}{U}(U - U_2)^2 - \frac{\chi}{\sigma}\frac{\gamma}{CC_2}(C - C_2)^2 + \frac{\eta_{CM}\rho_H + \chi\rho_M}{\eta_{CM}}(R_3 - 1)H.
\end{aligned}
$$

Then, if $R_3 \leq 1$ and by using inequality (4.1), we obtain that

$$
\frac{d\mathcal{L}_2}{dt} \leq 0
$$

for any

$$
U, H, C, M > 0.
$$

Moreover,

$$
\frac{d\mathcal{L}_2}{dt} = 0
$$

if

$$
U = U_2, \quad C = C_2, \quad \text{and} \quad (R_3 - 1)H = 0.
$$

The model's solutions converge to $\mathcal{H}_2'$ where

$$
U = U_2, \quad C = C_2
$$

and

$$
(R_3 - 1)H = 0. \tag{4.10}
$$

As a result, two cases arise:

(I) $R_3 = 1$. From Eq (2.1), we have

$$
\dot{U} = \alpha - \rho_U U_2 - \eta_{UH}U_2 H = 0 \implies H(t) = 0 \text{ for any } t. \tag{4.11}
$$

Equation (2.3) implies that

$$
\dot{C} = \gamma - \rho_C C_2 - \eta_{CM}C_2 M = 0 \implies M(t) = M_2 \text{ for any } t. \tag{4.12}
$$

Hence,

$$
\mathcal{H}_2' = \{EP_2\}.
$$

(II) $R_3 < 1$. Then, from Eq (4.10), we obtain $H = 0$. In addition, Eq (4.12) gives $M = M_2$ and, hence,

$$
\mathcal{H}_2' = \{EP_2\}.
$$

Consequently, by LP, EP_2 is GAS.

We demonstrate that if $R_3 > 1$, then EP_2 is unstable. By applying the Jacobian matrix in Eq (4.5), we can derive the characteristic equation at the equilibrium EP_2 as follows:

$$
\begin{aligned}
\Gamma(\Lambda) =\ & \eta_{CM}\rho_U\rho_M\Lambda^3 + \left(\gamma\eta_{CM}^2\rho_U + \rho_M(-\alpha\eta_{UH}\eta_{CM} + \eta_{CM}\rho_U\rho_H + \rho_U\chi\rho_M)\right)\Lambda^2 \\
& + \left(\gamma\eta_{CM}(-\alpha\eta_{UH}\eta_{CM} + \eta_{CM}\rho_U\rho_H + \rho_U\chi\rho_M) + \eta_{CM}\rho_U\left(\gamma\eta_{CM}\rho_M - \rho_C\rho_M^2\right)\right)\Lambda \\
& + (-\alpha\eta_{UH}\eta_{CM} + \eta_{CM}\rho_U\rho_H + \rho_U\chi\rho_M)\left(\gamma\eta_{CM}\rho_M - \rho_C\rho_M^2\right) \\
=\ & 0.
\end{aligned}
$$

Γ is continuous on $[0, \infty)$,

$$
\lim_{\Lambda\to\infty}\Gamma(\Lambda) = \infty
$$

and

$$
\begin{aligned}
\Gamma(0) =\ & \rho_C\rho_U\rho_M^2\left(\eta_{CM}\rho_H + x\rho_M\right)\left(1 - \frac{\alpha\eta_{UH}\eta_{CM}}{\rho_U\left(\eta_{CM}\rho_H + x\rho_M\right)}\right)\left(\frac{\gamma\eta_{CM}}{\rho_C\rho_M} - 1\right) \\
=\ & \rho_C\rho_U\rho_M^2\left(\eta_{CM}\rho_H + x\rho_M\right)\left(1 - R_3\right)\left(R_2 - 1\right).
\end{aligned}
$$

Since $R_2 > 1$ and $R_3 > 1$, then $\Gamma(0) < 0$. Hence, $\Gamma(\Lambda)$ has a positive root, and thus EP_2 is unstable.

This completes the proof. □

Theorem 4. *HTLV-1/HTLV-2 co-infection equilibrium, EP_3 is GAS if $R_3 > 1$ and $R_4 > 1$.*

Proof. Define $\mathcal{L}_3(U, H, C, M)$ as:

$$
\mathcal{L}_3 = U_3\mathcal{F}\left(\frac{U}{U_3}\right) + H_3\mathcal{F}\left(\frac{H}{H_3}\right) + \frac{\chi}{\sigma}C_3\mathcal{F}\left(\frac{C}{C_3}\right) + \frac{\chi}{\sigma}M_3\mathcal{F}\left(\frac{M}{M_3}\right).
$$

Calculating $\frac{d\mathcal{L}_3}{dt}$ as:

$$
\begin{aligned}
\frac{d\mathcal{L}_3}{dt} =\ & \left(1 - \frac{U_3}{U}\right)(\alpha - \rho_U U - \eta_{UH}UH) + \left(1 - \frac{H_3}{H}\right)(\eta_{UH}UH - \rho_H H - \chi HC) \\
& + \frac{\chi}{\sigma}\left(1 - \frac{C_3}{C}\right)(\gamma + \sigma HC - \rho_C C - \eta_{CM}CM) + \frac{\chi}{\sigma}\left(1 - \frac{M_3}{M}\right)(\eta_{CM}CM - \rho_M M).
\end{aligned}
$$

Then we obtain

$$
\begin{aligned}
\frac{d\mathcal{L}_3}{dt} =\ & \left(1 - \frac{U_3}{U}\right)(\alpha - \rho_U U) + \eta_{UH}U_3 H - \eta_{UH}H_3 U - \rho_H H + \rho_H H_3 + \chi H_3 C \\
& + \frac{\chi}{\sigma}\left(1 - \frac{C_3}{C}\right)(\gamma - \rho_C C) - \chi C_3 H + \frac{\chi\eta_{CM}}{\sigma}C_3 M - \frac{\chi\eta_{CM}}{\sigma}M_3 C - \frac{\chi\rho_M}{\sigma}M + \frac{\chi\rho_M}{\sigma}M_3.
\end{aligned}
$$

Using the equilibrium conditions

$$
\begin{cases}
\alpha = \rho_U U_3 + \eta_{UH}U_3 H_3, \\
\eta_{UH}U_3 H_3 = \rho_H H_3 + \chi H_3 C_3, \\
\gamma = \rho_C C_3 + \eta_{CM}C_3 M_3 - \sigma H_3 C_3, \\
C_3 = \frac{\rho_M}{\eta_{CM}}.
\end{cases}
$$

We obtain

$$
\begin{aligned}
\frac{d\mathcal{L}_3}{dt} ={}& \frac{-\rho_U}{U}(U-U_3)^2 - \frac{\chi}{\sigma}\frac{\rho_C}{C}(C-C_3)^2 + \left(1-\frac{U_3}{U}\right)\eta_{UH}U_3H_3 + \frac{\chi}{\sigma}\left(1-\frac{C_3}{C}\right)\eta_{CM}C_3M_3 \\
& - \chi\left(1-\frac{C_3}{C}\right)H_3C_3 + (\eta_{UH}U_3H_3 - \rho_H H_3 - \chi C_3 H_3)\frac{H}{H_3} + \frac{\chi\eta_{CM}}{\sigma}\left(C_3 - \frac{\rho_M}{\eta_{CM}}\right)M \\
& - \eta_{UH}U_3H_3\frac{U}{U_3} + \rho_H H_3 + \chi H_3 C_3\frac{C}{C_3} - \frac{\chi}{\sigma}\eta_{CM}M_3C_3\frac{C}{C_3} + \frac{\chi\rho_M}{\sigma}M_3 + \chi H_3 C_3 - \chi H_3 C_3 \\
={}& \frac{-\rho_U}{U}(U-U_3)^2 - \frac{\chi}{\sigma}\frac{\rho_C}{C}(C-C_3)^2 + \left(1-\frac{U_3}{U}\right)\eta_{UH}U_3H_3 \\
& + \frac{\chi}{\sigma}\left(1-\frac{C_3}{C}\right)\eta_{CM}C_3M_3 - \chi\left(1-\frac{C_3}{C}\right)H_3C_3\eta_{UH}U_3H_3\frac{U}{U_3} + \eta_{UH}U_3H_3 \\
& + \chi H_3 C_3\frac{C}{C_3} - \frac{\chi}{\sigma}\eta_{CM}M_3C_3\frac{C}{C_3} + \frac{\chi}{\sigma}\eta_{CM}C_3M_3 - \chi H_3 C_3.
\end{aligned}
$$

It follows that

$$
\begin{aligned}
\frac{d\mathcal{L}_3}{dt} ={}& \frac{-\rho_U}{U}(U-U_3)^2 - \frac{\chi}{\sigma}\frac{\rho_C}{C}(C-C_3)^2 + \left(2-\frac{U_3}{U}-\frac{U}{U_3}\right)\eta_{UH}U_3H_3 \\
& + \frac{\chi}{\sigma}\left(2-\frac{C_3}{C}-\frac{C}{C_3}\right)\eta_{CM}C_3M_3 - \chi\left(2-\frac{C_3}{C}-\frac{C}{C_3}\right)H_3C_3 \\
={}& \frac{-\rho_U}{U}(U-U_3)^2 - \frac{\chi}{\sigma}\frac{\rho_C}{C}(C-C_3)^2 - \frac{\eta_{UH}}{U}(U-U_3)^2 H_3 \\
& - \frac{\chi}{\sigma}\frac{\eta_{CM}}{C}(C-C_3)^2 M_3 + \frac{\chi}{C}(C-C_3)^2 H_3 \\
={}& \frac{-\alpha}{U}(U-U_3)^2 - \frac{\chi}{\sigma}\frac{\gamma}{C}(C-C_3)^2.
\end{aligned}
$$

Therefore, if $R_3 > 1$ and $R_4 > 1$, and by applying inequality (4.1), we deduce that

$$
\frac{d\mathcal{L}_3}{dt} \le 0
$$

for all

$$
U, H, C, M > 0.
$$

In addition,

$$
\frac{d\mathcal{L}_3}{dt} = 0
$$

if

$$
U = U_3 \quad \text{and} \quad C = C_3.
$$

Solutions of models (2.1)–(2.4) converge to $\mathcal{H}'_4$, where

$$
U = U_3 \quad \text{and} \quad C = C_3.
$$

It follows that

$$
\dot{U} = \dot{C} = 0,
$$

and then Eqs (2.1) and (2.3) give

$$\dot{U} = \alpha - \rho_U U_3 - \eta_{UH} U_3 H = 0 \implies H(t) = H_3 \quad \text{for any } t,$$
$$\dot{C} = \gamma + \sigma H_3 C_3 - \rho_C C_3 - \eta_{CM} C_3 M = 0 \implies M(t) = M_3 \quad \text{for any } t.$$

Thus, by LP

$$\mathcal{H}_3' = \{EP_3\}$$

and EP_3 is GAS.

This completes the proof. $\qquad\square$

Table 2 summarizes the conditions for the existence and global stability of each equilibrium in the models (2.1)–(2.4).

Table 2. Criteria for the existence and global stability of the equilibria in the models (2.1)–(2.4).

Equilibrium	Existence condition	Stability condition
$EP_0 = (U_0, 0, C_0, 0)$	-	$R_1 \le 1$ and $R_2 \le 1$
$EP_1 = (U_1, H_1, C_1, 0)$	$R_1 > 1$	$R_1 > 1$ and $R_4 \le 1$
$EP_2 = (U_2, 0, C_2, M_2)$	$R_2 > 1$	$R_2 > 1$ and $R_3 \le 1$
$EP_3 = (U_3, H_3, C_3, M_3)$	$R_3 > 1, R_4 > 1$	$R_3 > 1$ and $R_4 > 1$

Remark 2. Investigating the memory effects and hereditary properties on our model's behavior using fractional differential equations (FDEs) offers a compelling research direction. FDEs are particularly effective in representing memory effects and non-local interactions, which are crucial in biological [46] and epidemiological systems [47, 48]. While our study focuses on the integer-order version, extending the model to a fractional-order system could offer deeper insights into the long-term behavior of the system, particularly in capturing the persistence of infection or addiction-related processes. In recent years, the Lyapunov method has gained significant attention for studying the global stability of FDE models [49]. The Lyapunov functions constructed in this section are essential for examining a fractional model describing HTLV-1 and HTLV-2 co-dynamics.

5. Numerical simulations

The suggested model systems (2.1)–(2.4) are subjected to numerical simulation in order to acquire insights into dynamical features, hence enhancing our comprehension of how control approaches impact the dynamics of infectious disease transmission. First, the stability characteristics of the infectious model are examined.

5.1. Numerical simulations for systems (2.1)–(2.4)

This subsection provides numerical simulations based on the parameter values listed in Table 1 to visually represent the analytical results established in Theorems 1–4. We employed the ode45 solver in MATLAB to numerically solve the ordinary differential equation model. To establish the global stability of the system's equilibria, we show that its solutions converge to a specific equilibrium point,

irrespective of the initial conditions. Given the scarcity of real-world data on initial infections with HTLV-1 and HTLV-2, we consider three distinct initial values as follows:

$$\textbf{IP.1: } U(0) = 300, \quad H(0) = 0.1, \quad C(0) = 100, \quad M(0) = 30.$$
$$\textbf{IP.2: } U(0) = 400, \quad H(0) = 0.05, \quad C(0) = 150, \quad M(0) = 20.$$
$$\textbf{IP.3: } U(0) = 500, \quad H(0) = 0.01, \quad C(0) = 200, \quad M(0) = 10.$$

We perform the numerical simulation by choosing the parameters η_{UH} and η_{CM} in the following scenarios:

Scenario-1: η_{UH} and η_{CM} are set at 0.005 and 0.0005, respectively. Our findings indicate that with these values

$$R_1 = 0.74 < 1 \quad \text{and} \quad R_2 = 0.56 < 1.$$

The paths shown in Figure 2 originating from the three points all converge to the equilibrium point

$$EP_0 = (1000, 0, 333.33, 0).$$

This demonstrates that EP_0 is GAS as provided in Theorem 1. Consequently, the HTLV-1 and HTLV-2 will be eradicated by this process.

(a) Healthy CD4$^+$ T cells

(b) HTLV-1-infected CD4$^+$ T cells

(c) Healthy CD8$^+$ T cells

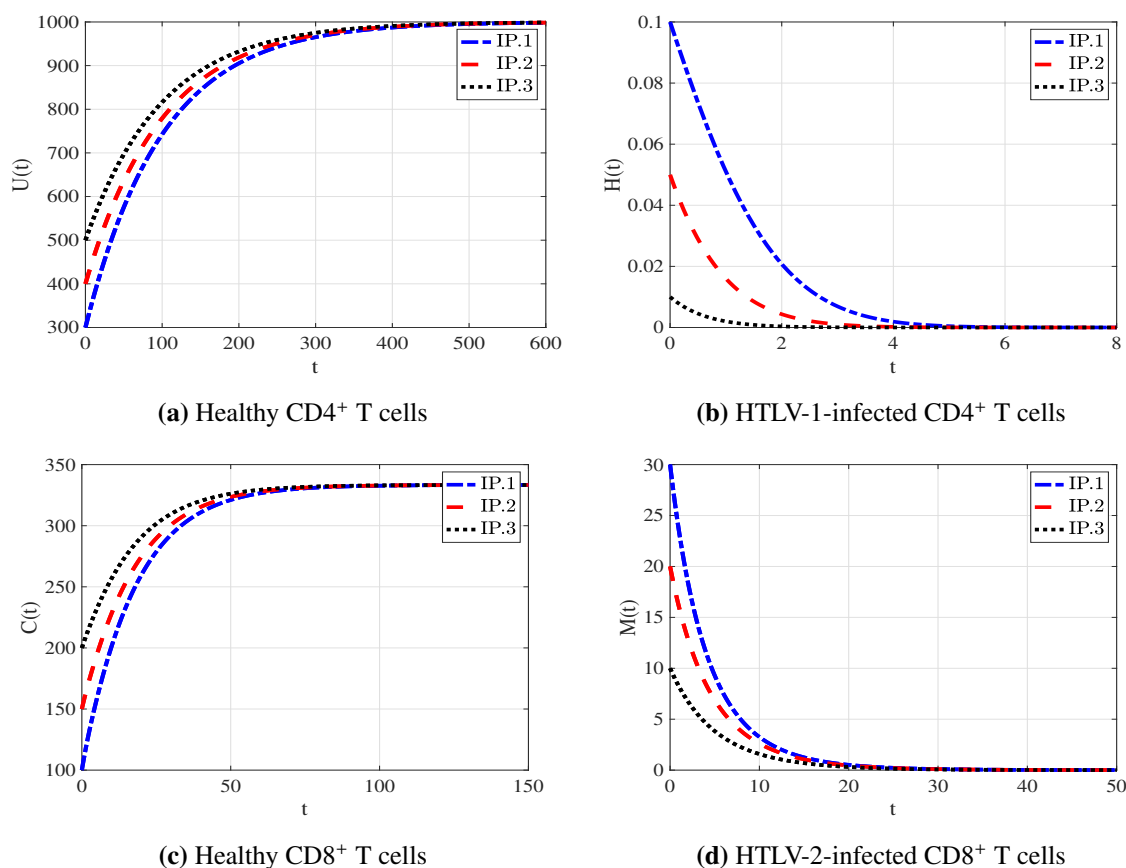**(d)** HTLV-2-infected CD8$^+$ T cells

Figure 2. The numerical simulations of systems (2.1)–(2.4) when $R_1 \leq 1$ and $R_2 \leq 1$ illustrate that the infection-free equilibrium $EP_0 = (1000, 0, 333.33, 0)$ is GAS (Scenario-1).

Scenario-2: η_{UH} and η_{CM} are set at 0.01 and 0.0005, respectively. This means that

$$R_1 = 1.49 > 1$$

and

$$R_4 = 0.77 < 1.$$

The results depicted in Figure 3 illustrate how the solutions reach the equilibrium point

$$EP_1 = (923.91, 0.08, 459.46, 0).$$

In this scenario, Theorem 2 aligns with the findings. This situation exemplifies the effects of HTLV-1 infection without HTLV-2 on an individual health. It is evident that HTLV-1 has caused a decrease in CD4$^+$ T cell counts and an increase in CD8$^+$ T cell levels.

(a) Healthy CD4$^+$ T cells

(b) HTLV-1-infected CD4$^+$ T cells

(c) Healthy CD8$^+$ T cells

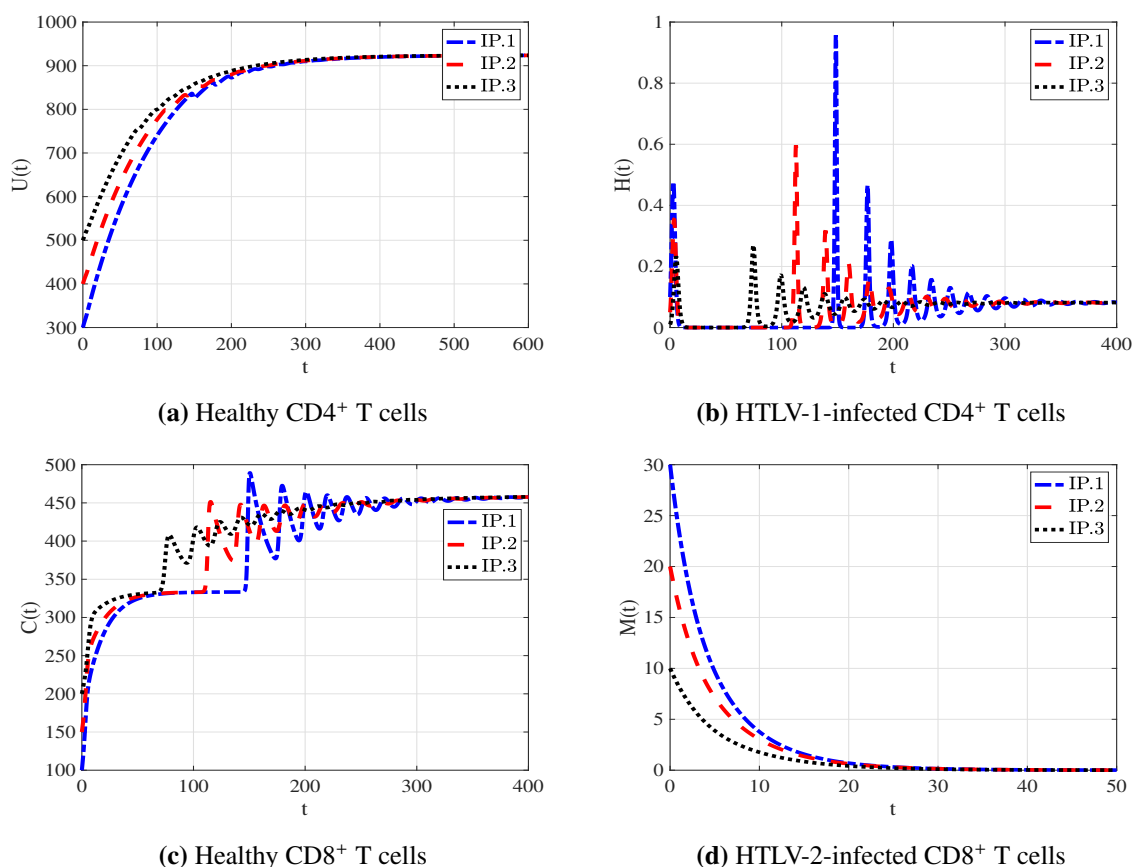(d) HTLV-2-infected CD8$^+$ T cells

Figure 3. The numerical simulations of systems (2.1)–(2.4) when $R_1 > 1$ and $R_4 \leq 1$ illustrate that the HTLV-1 mono-infection equilibrium $EP_1 = (923.91, 0.08, 459.46, 0)$ is GAS (Scenario-2).

Scenario-3: The values of η_{UH} and η_{CM} are 0.001 and 0.002, respectively. Next, we calculate

$$R_2 = 2.22 > 1$$

and

$$R_3 = 0.33 < 1.$$

It is clear that the criteria outlined in Table 2 are satisfactorily met. In Figure 4 we can observe how the solutions converge towards the equilibrium point

$$EP_2 = (1000, 0, 150, 36.67)$$

thereby confirming Theorem 3. This scenario illustrates the progression when an individual is solely infected with HTLV-2. Even though CD4$^+$ T cell levels remain normal, it is evident that HTLV-2 has caused a decrease in CD8$^+$ T cell counts.

(a) Healthy CD4$^+$ T cells

(b) HTLV-1-infected CD4$^+$ T cells

(c) Healthy CD8$^+$ T cells

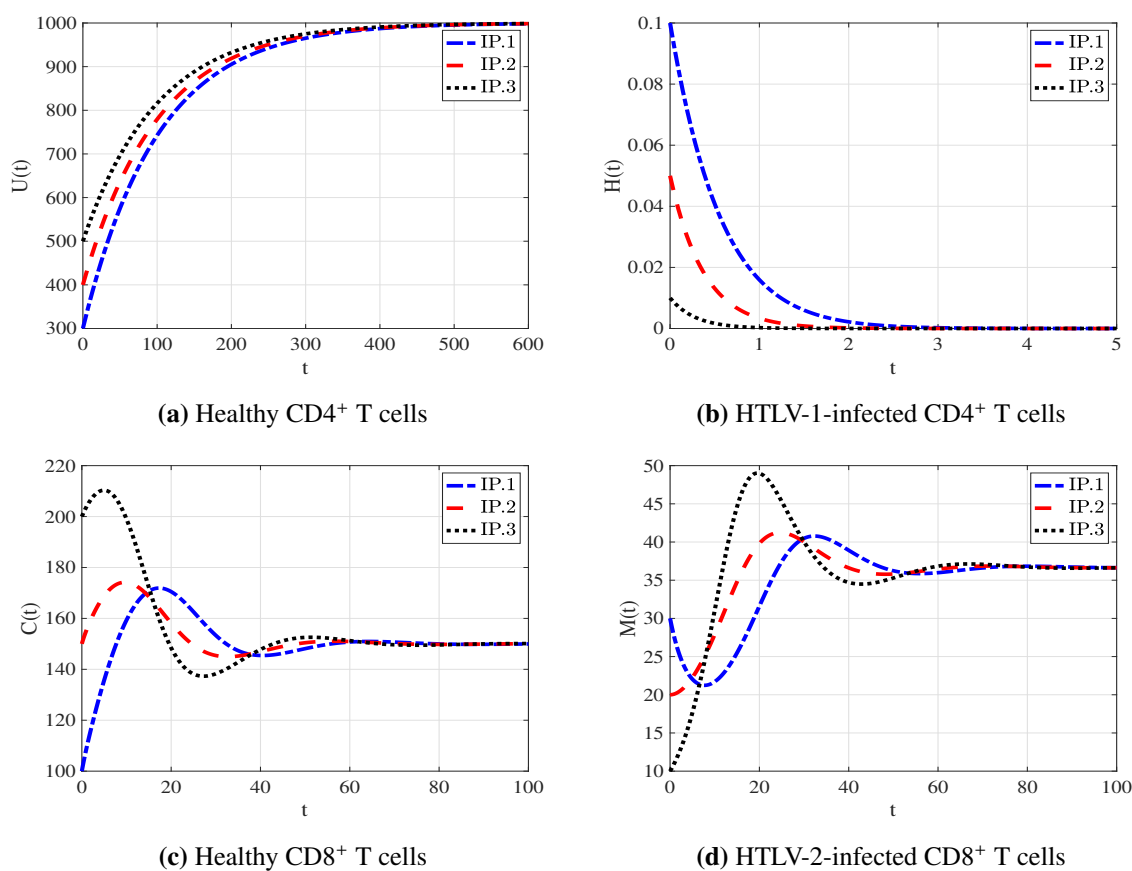(d) HTLV-2-infected CD8$^+$ T cells

Figure 4. The numerical simulations of systems (2.1)–(2.4) when $R_2 > 1$ and $R_3 \leq 1$ illustrate that the HTLV-2 mono-infection equilibrium $EP_2 = (1000, 0, 150, 36.67)$ is GAS (Scenario-3).

Scenario-4: η_{UH} is 0.003, while η_{CM} is 0.004. After that, we calculate

$$R_3 = 1.94 > 1$$

and

$$R_4 = 2.14 > 1.$$

The conditions specified in Table 2 are clearly met. As depicted in Figure 5, the solutions approach the equilibrium

$$EP_3 = (516.67, 3.12, 75, 207.58)$$

and confirm Theorem 4. This scenario illustrates the consequences of co-infection with both HTLV-1 and HTLV-2 viruses in an individual. The quantities of healthy CD4$^+$ T cells and CD8$^+$ T cells decline, resulting in a weakening of the patient's immune system.

(a) Healthy CD4$^+$ T cells

(b) HTLV-1-infected CD4$^+$ T cells

(c) Healthy CD8$^+$ T cells

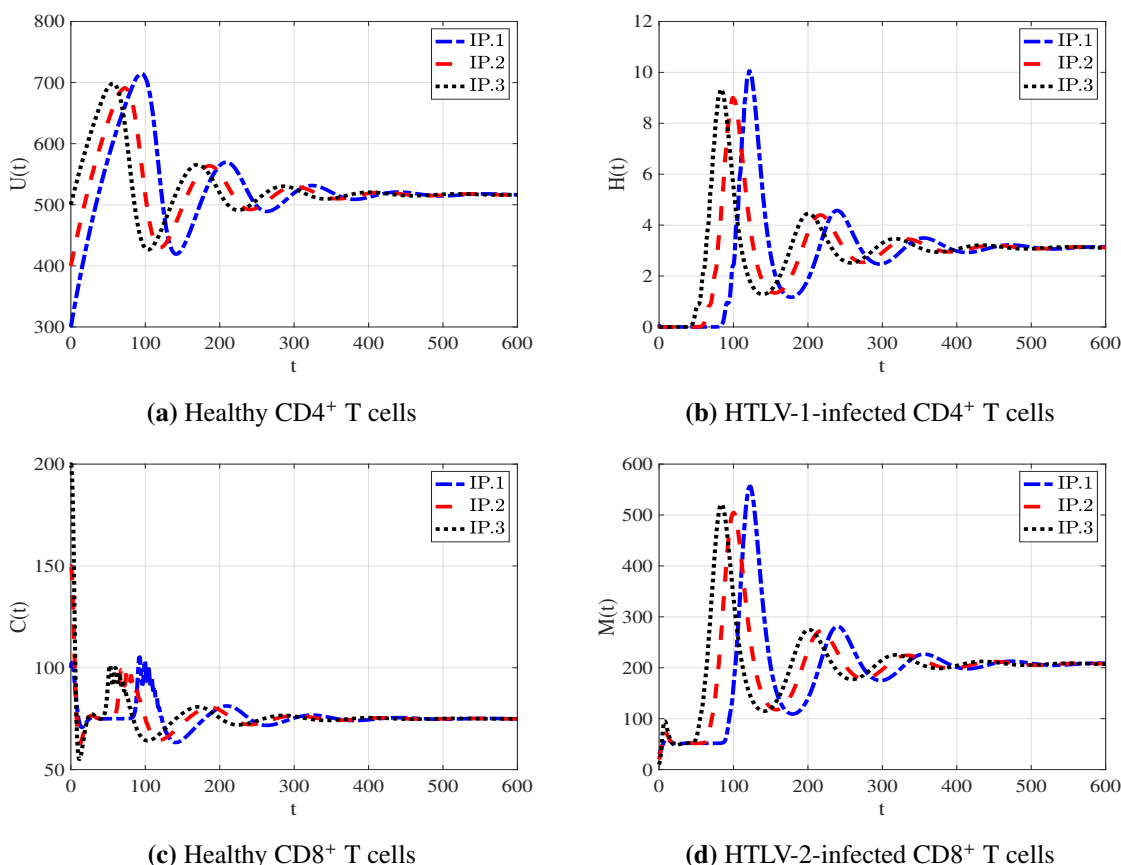**(d)** HTLV-2-infected CD8$^+$ T cells

Figure 5. The numerical simulations of systems (2.1)–(2.4) when $R_3 > 1$ and $R_4 > 1$ illustrate that the HTLV-1/HTLV-2 co-infection equilibrium $EP_3 = (516.67, 3.12, 75, 207.58)$ is GAS (Scenario-4).

To provide additional verification, an analysis of the local stability is conducted for all equilibria. The Jacobian matrix $\mathcal{J}$, which depends on the variables U, H, C, and M, is calculated in Eq (4.5). To determine the stability of each equilibrium, we compute the eigenvalues λ_k, where $k = 1, \ldots, 4$ of $\mathcal{J}$. An equilibrium point is considered stable if all eigenvalues have a real part less than zero, denoted as

$$\mathrm{Re}(\lambda_k) < 0$$

for all $k = 1, 2, 3, 4$. By calculating the nonnegative EPs and utilizing the parameter values specified in Scenarios 1–4, we can determine the eigenvalues associated with all equilibria. Table 3 provided a comprehensive overview of the positive equilibria and the real part of the eigenvalues.

Table 3. Local stability of EPs

Scenario	Equilibrium	$\mathrm{Re}(\lambda_k) < 0, k = 1, 2, 3, 4$	Stability
1	$EP_0 = (1000, 0, 333.33, 0)$	$(-1.72, -0.13, -0.06, -0.01)$	stable
2	$EP_0 = (1000, 0, 333.33, 0)$	$(3.28, -0.13, -0.06, -0.01)$	unstable
	$EP_1 = (923.91, 0.08, 459.46, 0)$	$(-0.02, -0.02, -0.07, -0.01)$	stable
3	$EP_0 = (1000, 0, 333.33, 0)$	$(-5.72, 0.37, -0.06, -0.01)$	unstable
	$EP_2 = (1000, 0, 150, 36.67)$	$(-2.05, -0.07, -0.07, -0.01)$	stable
4	$EP_0 = (1000, 0, 333.33, 0)$	$(-3.72, 1.03, -0.06, -0.01)$	unstable
	$EP_2 = (1000, 0, 75, 51.67)$	$(1.45, -0.13, -0.13, -0.01)$	unstable
	$EP_3 = (516.67, 3.12, 75, 207.58)$	$(-0.13, -0.13, -0.01, -0.01)$	stable

5.2. Sensitivity analysis

Sensitivity analysis is important for understanding systems by showing how model outcomes are affected by different parameters [50]. It helps enhance our grasp of model research. Sensitivity analysis evaluates how biological reactions change when parameters are adjusted, helping pinpoint the factors influencing model results [51]. Several methods of sensitivity analysis were introduced for biological models [51]. We apply derivative-based sensitivity analysis to our system. By computing the derivatives with respect to model parameters, we can analytically determine the indices. In our study, we examine the effect of R_1 and R_2 on the stability of disease-free infection equilibrium using sensitivity analysis. The normalized forward sensitivity index for R_i (where $k = 1, 2$) is expressed as follows:

$$S_\beta^{R_k} = \frac{\partial R_k}{\partial \beta} \times \frac{\beta}{R_k}, \tag{5.1}$$

where β represents a given parameter.

5.2.1. Sensitivity analysis for R_1

Applying form (5.1) and using the parameter values provided in Table 1, we calculated the sensitivity indices of R_1 with respect to each parameter, as presented in Table 4.

Table 4. Sensitivity index for R_1.

Parameters β	α	η_{UH}	ρ_C	ρ_U	χ	γ	ρ_H
Value of $S_\beta^{R_1}$	1	1	0.9970	-1	-0.9970	-0.9970	-0.0030

The sensitivity index values for R_1 with respect to the parameters are given in Table 1. Based on the presented sensitivity indices in Table 4, we observe that:

- The parameters α, η_{UH}, and ρ_C show positive sensitivity indices, suggesting that changes in these parameters will lead to corresponding increases or decreases in the basic reproduction number R_1 for HTLV-1 mono-infection. Among them, α and η_{UH} exhibit the highest positive sensitivity indices.

- On the other hand, ρ_U, χ, γ, and ρ_H have a negative influence on R_1. As a result, an increase in these values will lead to a reduction in the value of R_1. Among these parameters, ρ_U, χ, and γ show greater significance compared to ρ_H.

5.2.2. Sensitivity analysis for R_2

Using Eq (5.1), we can calculate the sensitivity indices of R_2 with respect to each parameter as shown in Table 5. It is clear that the sensitivity analysis of R_2 is independent of the parameter values, as the sensitivity to any parameter is consistently either 1 or -1. The signs presented in Table 5 help us understand how each parameter contributes to the sensitivity analysis as:

- The values of parameters γ and η_{CM} positively influence the growth of HTLV-2 in the body, suggesting their role in its proliferation.

- In contrast, parameters ρ_C and ρ_M are associated with reducing the transmission rate of HTLV-2 within humans.

Table 5. Sensitivity index of R_2.

Parameters β	γ	η_{CM}	ρ_C	ρ_M
Value of $S_\beta^{R_2}$	1	1	-1	-1

5.3. HTLV-1 and HTLV-2 co-dynamics under the effect of stimulation rate of CD8$^+$ T cells

This subsection examines the impact of the stimulated rate constant of CD8$^+$ T cells, denoted as σ, on the system dynamics described by (2.1)–(2.4). In order to investigate the impact of CD8$^+$ T cells on the model's solutions, we hold the values of

$$\eta_{UH} = 0.003$$

and

$$\eta_{CM} = 0.004$$

while varying the parameter σ. By choosing the following initial point:

IP.4: $U(0) = 500, \quad H(0) = 2, \quad C(0) = 50, \quad M(0) = 500.$

From Figure 6, we observe that as σ increases, the quantities of healthy CD4$^+$ T and CD8$^+$ T cells remain increased. Moreover, the number of HTLV-1-infected CD4$^+$ T cells decreases.

It is also important to note that an increase in CD8$^+$ T cells will increase the number of HTLV-2-infected CD8$^+$ T cells. Clearly, enhanced CD8$^+$ T cell stimulation helps control HTLV-1 infection while also promoting the spread of HTLV-2 infection. Due to the fact that R_1 and R_2 are independent of σ, increasing σ does not result in the attainment of EP_0. To boost CD8$^+$ T cell stimulation, the parameter σ can be substituted with $(1 + \epsilon_{IT})\sigma$, where $\epsilon_{IT} \in [0, 1]$ denotes the drug efficacy of immunotherapy (IT), which enhances the proliferation of CD8$^+$ T cells in infected individuals through the subcutaneous administration of IL-2, promoting their activation and differentiation [20].
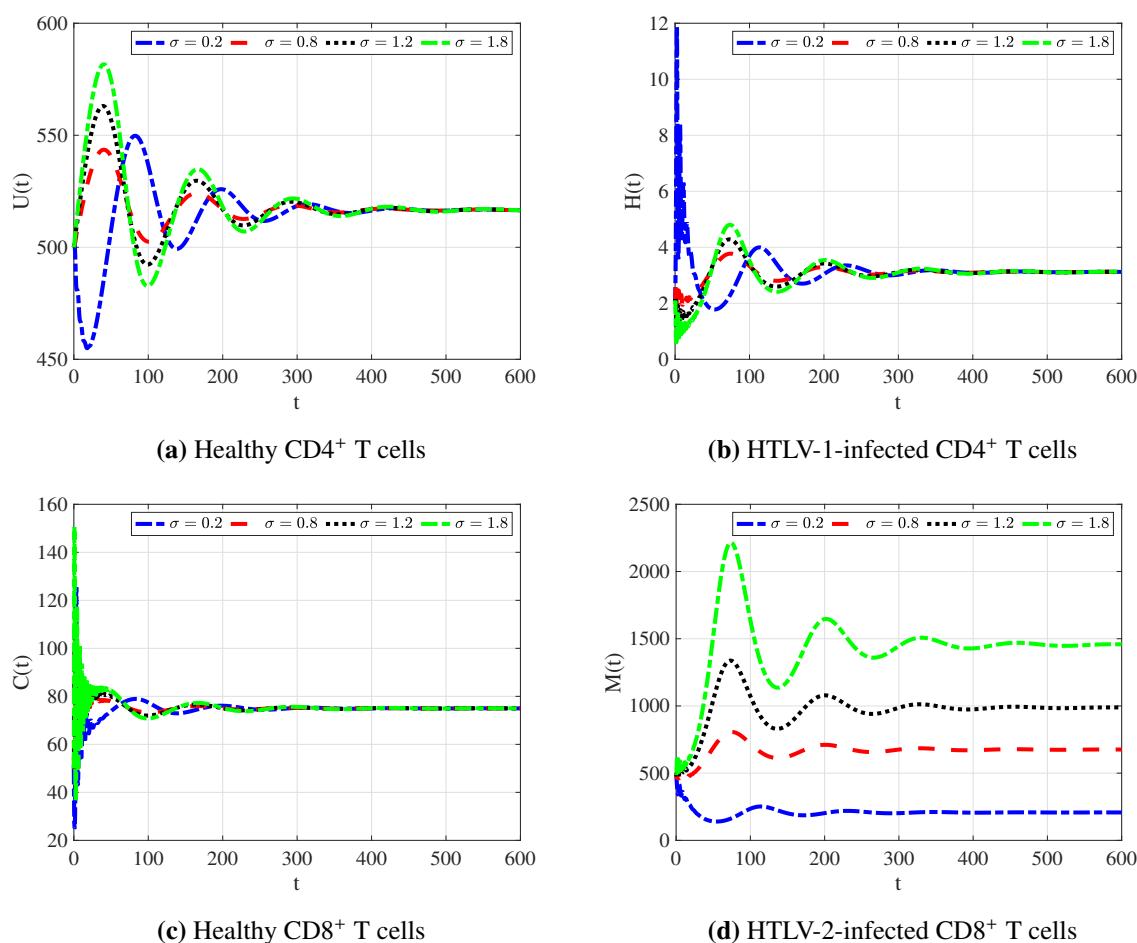
(a) Healthy CD4$^+$ T cells

(b) HTLV-1-infected CD4$^+$ T cells

(c) Healthy CD8$^+$ T cells

(d) HTLV-2-infected CD8$^+$ T cells

Figure 6. Effect of stimulation rate of CD8$^+$ T cells on the HTLV-1 and HTLV-2 co-infection dynamics.

5.4. Impact of infection rates η_{UH} and η_{CM} on the HTLV1 and HTLV-2 co-dynamics

In this part, we explore the impact of infection rates η_{UH} and η_{CM} on the HTLV1 and HTLV-2 co-dynamics. To demonstrate the impact of η_{UH} on the HTLV1 and HTLV-2 co-dynamics, we set

$$\eta_{CM} = 0.004.$$

We consider different values of η_{UH} as

$$\eta_{UH} = 0.003, \ 0.009, \ 0.03, \ 0.09$$

and numerically solve systems (2.1)–(2.4) together with the following initial point:

IP.5: $U(0) = 200, \ H(0) = 2, \ C(0) = 50, \ M(0) = 200.$

Figure 7 reveals a correlation in which an increase in η_{UH} leads to a reduction in the number of healthy CD4$^+$ T cells, while the behavior of healthy CD8$^+$ T cells does not change too much. At the same time, populations of HTLV-1-infected CD4$^+$ T cells and HTLV-2-infected CD8$^+$ T cells increase.

In this context, raising η_{UH} may increase the risk of HTLV-2 infection. To reduce the HTLV-1 infection, the parameter η_{UH} can be replaced with $(1 - \epsilon_{\text{RTI}})\eta_{UH}$, where $\epsilon_{\text{RTI}} \in [0, 1]$ represents the drug efficacy of reverse-transcriptase inhibitors (RTI) like zidovudine, which effectively block the virus from spreading throughout the body [20, 52].
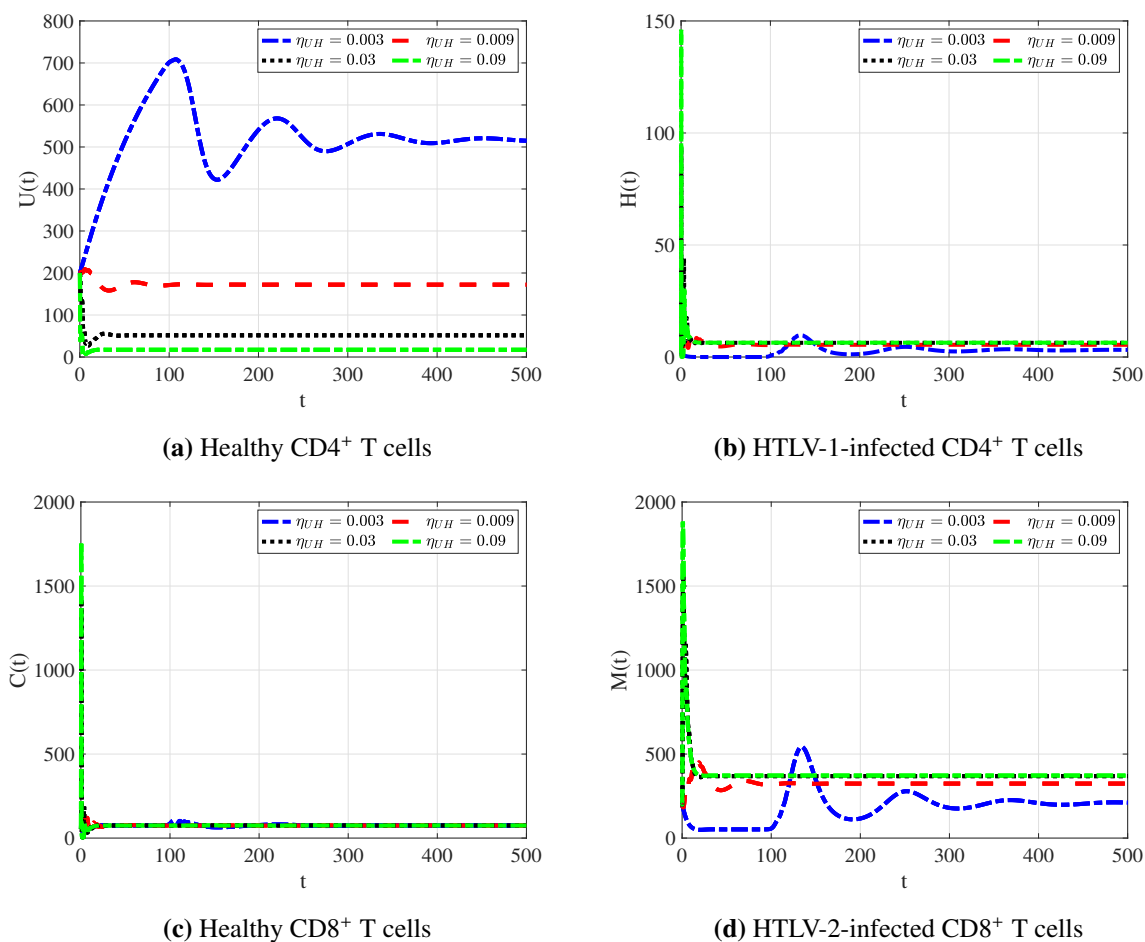

(a) Healthy CD4+ T cells

(b) HTLV-1-infected CD4+ T cells

(c) Healthy CD8+ T cells

(d) HTLV-2-infected CD8+ T cells

Figure 7. Impact of the infection rate η_{UH} on the HTLV-1 and HTLV-2 co-infection dynamics.

To demonstrate the effect of η_{CM} on the HTLV1 and HTLV-2 co-dynamics, we set

$$\eta_{UH} = 0.003.$$

We examine different values of

$$\eta_{CM} : \eta_{CM} = 0.004, \ 0.006, \ 0.008, \ 0.01,$$

and numerically solve systems (2.1)–(2.4) with the following initial point:

IP.6: $U(0) = 200, \ H(0) = 0.5, \ C(0) = 80, \ M(0) = 80.$

Analysis of Figure 8 shows a correlation where an increase in η_{CM} results in a decrease in both healthy CD4+ T cells and healthy CD8+ T cells. At the same time, the populations of HTLV-1-infected CD4+

T cells and HTLV-2-infected CD8$^+$ T cells increase. In this context, raising η_{CM} may increase the HTLV-1 progression.

(a) Healthy CD4$^+$ T cells

(b) HTLV-1-infected CD4$^+$ T cells

(c) Healthy CD8$^+$ T cells
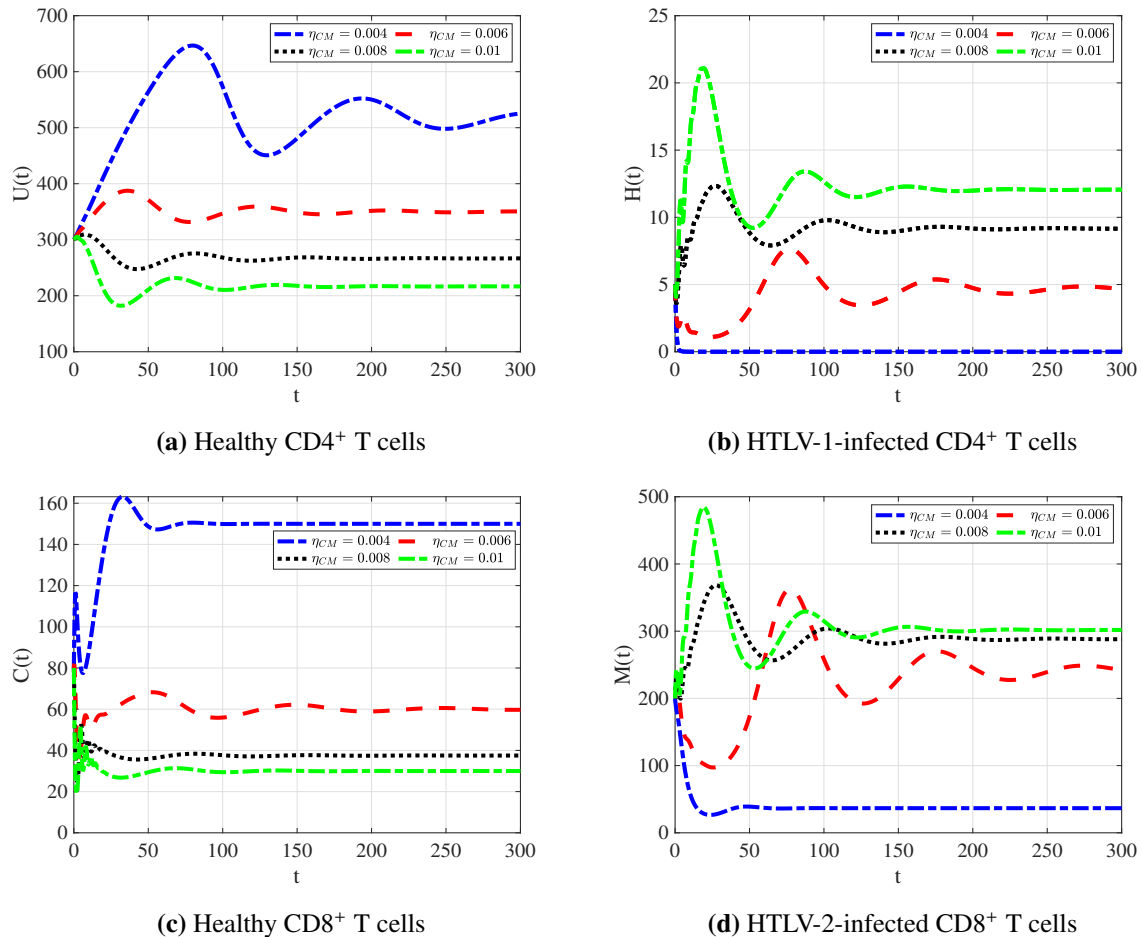
(d) HTLV-2-infected CD8$^+$ T cells

Figure 8. Impact of the infection rate η_{CM} on the HTLV-1 and HTLV-2 co-infection dynamics.

6. Discussion

Since HTLV-1 and HTLV-2 are closely linked to various health concerns and share transmission routes, they are especially common in high-risk populations, particularly among individuals who use injection drugs. Therefore, understanding the within-host co-dynamics of HTLV-1 and HTLV-2 is crucial. In this paper, we develop a model to describe the dynamics of HTLV-1 and HTLV-2 co-infection. A summary of the equilibria in our model is as follows:

(I) Disease-free equilibrium. EP_0: this equilibrium always exists and is GAS when

$$R_1 \leq 1 \quad \text{and} \quad R_2 \leq 1.$$

In this scenario, both HTLV-1 and HTLV-2 will be eradicated from the system. While there is no definitive cure for HTLV infections, treatment mainly focuses on managing associated conditions

such as ATL and HAM/TSP using chemotherapy, corticosteroids, interferon, and supportive care. If antiviral drugs for HTLV-1 and HTLV-2 become available, it may be possible to achieve

$$R_1 \le 1 \quad \text{and} \quad R_2 \le 1$$

by adjusting the parameters η_{UH} and η_{CM}. Specifically, these parameters can be replaced with $(1 - \epsilon_{\text{RTI-HTLV-1}})\eta_{UH}$ and $(1 - \epsilon_{\text{RTI-HTLV-2}})\eta_{UH}$ where $\epsilon_{\text{RTI-HTLV-1}} \in [0, 1]$, and $\epsilon_{\text{RTI-HTLV-2}} \in [0, 1]$ represent the efficacy of RTI drugs for HTLV-1 and HTLV-2, respectively. Then R_1 and R_2 become

$$R_1 = \frac{(1 - \epsilon_{\text{RTI-HTLV-1}})\,\alpha\eta_{UH}\rho_C}{\rho_U\,(\rho_H\rho_C + \chi\gamma)},$$
$$R_2 = \frac{(1 - \epsilon_{\text{RTI-HTLV-2}})\,\gamma\eta_{CM}}{\rho_M\rho_C}.$$

Therefore, $R_1 \le 1$ when

$$\epsilon^{\min}_{\text{RTI-HTLV-1}} \le \epsilon_{\text{RTI-HTLV-1}} \le 1,$$

$R_2 \le 1$ when

$$\epsilon^{\min}_{\text{RTI-HTLV-2}} \le \epsilon_{\text{RTI-HTLV-2}} \le 1,$$

where

$$\epsilon^{\min}_{\text{RTI-HTLV-1}} = \max\left\{0, 1 - \frac{\rho_U\,(\rho_H\rho_C + \chi\gamma)}{\alpha\eta_{UH}\rho_C}\right\},$$
$$\epsilon^{\min}_{\text{RTI-HTLV-2}} = \max\left\{0, 1 - \frac{\rho_M\rho_C}{\gamma\eta_{CM}}\right\}.$$

In this context, $\epsilon^{\min}_{\text{RTI-HTLV-1}}$ and $\epsilon^{\min}_{\text{RTI-HTLV-2}}$ represent the minimum drug efficacies necessary to stabilize EP_0 and eliminate the co-infection from the host. By treating drug efficacies as control variables, optimal control theory can be applied to develop treatment strategies that minimize both the cost of the drugs and their associated side effects [24].

(II) HTLV-1 single infection equilibrium point. EP_1: this equilibrium exists if $R_1 > 1$ and is GAS if $R_4 \le 1$. This scenario represents an individual infected only with HTLV-1. This likely occurs when $\epsilon_{\text{RTI-HTLV-1}}$ is insufficient to eliminate the HTLV-1 infection, whereas $\epsilon_{\text{RTI-HTLV-2}}$ is effective in clearing HTLV-2.

(III) HTLV-2 single infection equilibrium point. EP_2: this equilibrium exists if $R_2 > 1$ and is GAS if $R_3 \le 1$. It describes a situation where an individual is infected only with HTLV-2. This situation may arise when $\epsilon_{\text{RTI-HTLV-2}}$ fails to eradicate HTLV-2, whereas $\epsilon_{\text{RTI-HTLV-1}}$ is sufficient to eliminate HTLV-1.

(IV) HTLV-1 and HTLV-2 co-infection equilibrium point. EP_3: this equilibrium point exists and is GAS if

$$R_3 > 1 \quad \text{and} \quad R_4 > 1.$$

It represents an individual co-infected with both HTLV-1 and HTLV-2. Our findings indicate that co-infection with both HTLV-1 and HTLV-2 leads to a decrease in the number of healthy CD4$^+$

and CD8$^+$ T cells, while the number of HTLV-1-infected CD4$^+$ T cells and HTLV-2-infected CD8$^+$ T cells increases, ultimately compromising the patient's immune response. This may elevate the risk associated with both infections.

A key limitation of our study is the inability to estimate the model's parameter values using real-world data. This challenge arises due to several factors: (i) the scarcity of available data on HTLV-1 and HTLV-2 co-infection; (ii) the limited number of studies on this topic, making comparisons less reliable; and (iii) the difficulty in obtaining clinical data from patients infected with both viruses.

7. Conclusions and future perspectives

In this study, we examined a mathematical model that captures the population dynamics of two HTLV strains, HTLV-1 and HTLV-2, which infect distinct target cells specifically CD4$^+$ T cells and CD8$^+$ T cells, both crucial to the human immune system. Our model captures the interactions among four components: healthy CD4$^+$ T cells, healthy CD8$^+$ T cells, HTLV-1-infected CD4$^+$ T cells, and HTLV-2-infected CD8$^+$ T cells. We have provided preliminary results regarding the boundedness and non-negativity of the solutions to the model. We then determined that the models possess four EPs. Through the application of LaSalle's invariance principle and the construction of suitable Lyapunov functions, we identified four threshold parameters (R_1, R_2, R_3, R_4) that determine the global stability of the equilibrium points. To validate these theoretical results, numerical simulations were carried out. We found, a close match between the numerical and theoretical outcomes. A sensitivity analysis was conducted to evaluate the impact of the model's parameters on the basic reproduction numbers R_1 and R_2. The key findings emerged from the analysis:

- The model examined encompasses several clinical scenarios, including a patient who has recovered from both HTLV-1 and HTLV-2 infections, an individual with chronic HTLV-1 mono-infection, another with chronic HTLV-2 mono-infection, and a patient with persistent co-infection of both viruses.

- Enhanced stimulation of CD8$^+$ T cells helps control HTLV-1 infection, while simultaneously promoting the spread of HTLV-2 infection. Numerous studies provide valuable insights into diverse approaches for boosting CD8$^+$ T cell activation and their potential use in therapy (see, e.g., [53, 54]). CD8$^+$ T cell stimulation can be enhanced through immunotherapy, which involves promoting the proliferation of CD8$^+$ T cells in infected individuals via subcutaneous injection of IL-2, thereby activating and differentiating the T cells [20].

- The coinfection with HTLV-1 and HTLV-2 may increase the risk of both viruses. Immune system dysregulation caused by both viruses could contribute to a higher inflammatory state, possibly worsening neurological symptoms.

Modeling the interactions between HTLV-1 and HTLV-2 has provided crucial insights into their pathogenesis and has also played a role in shaping guidelines for more effective treatment strategies for co-infection.

Our proposed model can be expanded in several directions:

(i) Incorporating a generalized incidence function $\Psi(U, H)$ that encompasses various forms, such as saturated incidence, Beddington-DeAngelis incidence, and Crowley-Martin incidence [41];

(ii) Extending the model using partial differential equations to account for cellular mobility;

(iii) Employing fractional differential equations to capture the influence of immunological memory [48]. Future research could explore incorporating the impact of various drug therapies into the model.

Moreover, we aim to compare the model's outcomes with data from infected patients to validate its predictions.

Author contributions

E. A. Almohaimeed: conceptualization, formal analysis; A. M. Elaiw: investigation, formal analysis; A. D. Hobiny: methodology, writing original draft. All authors have read and agreed to the published version of the manuscript.

Use of Generative-AI tools declaration

The authors declare they have not used Artificial Intelligence (AI) tools in the creation of this article.

Acknowledgments

Conflict of interest

The authors declare that they have no conflicts of interest.

References

1. M. T. Raza, S. Mizan, F. Yasmin, A. S. Akash, S. M. Shahik, Epitope-based universal vaccine for human T-lymphotropic virus-1 (HTLV-1), *PloS One*, **16** (2021), e0248001. https://doi.org/10.1371/journal.pone.0248001

2. K. S. Jones, K. Fugo, C. Petrow-Sadowski, Y. Huang, D. C. Bertolette, I. Lisinski, et al., Human T-cell leukemia virus type 1 (HTLV-1) and HTLV-2 use different receptor complexes to enter T cells, *J. Virol.*, **80** (2006), 8291–8302. https://doi.org/10.1128/JVI.00389-06

3. F. Marino-Merlo, E. Balestrieri, C. Matteucci, A. Mastino, S. Grelli, B. Macchi, Antiretroviral therapy in HTLV-1 infection: an updated overview, *Pathogens*, **9** (2020), 342. https://doi.org/10.3390/pathogens9050342

4. D. M. Solorzano-Salazar, A. Hernández-Vásquez, F. J. Visconti-Lopez, D. Azañedo, Research on HTLV-1 and HTLV-2 in latin America and the Caribbean over the last ten years, *Heliyon*, **9** (2023), e13800. https://doi.org/10.1016/j.heliyon.2023.e13800

5. M. P. Martinez, J. Al-Saleem, P. L. Green, Comparative virology of HTLV-1 and HTLV-2, *Retrovirology*, **16** (2019), 21. https://doi.org/10.1186/s12977-019-0483-0

6. A. Gessain, O. Cassar, Epidemiological aspects and world distribution of HTLV-1 infection, *Front. Microbiol.*, **3** (2012), 388. https://doi.org/10.3389/fmicb.2012.00388

7. E. L. Murphy, O. Cassar, A. Gessain, Estimating the number of HTLV-2 infected persons in the world, *Retrovirology*, **12** (2015), O5. https://doi.org/10.1186/1742-4690-12-S1-O5

8. G. Schierhout, S. McGregor, A. Gessain, L. Einsiedel, M. Martinello, J. Kaldor, Association between HTLV-1 infection and adverse health outcomes: a systematic review and meta-analysis of epidemiological studies, *Lancet Infect. Dis.*, **20** (2020), 133–143. https://doi.org/10.1016/S1473-3099(19)30402-5

9. M. A. Nowak, R. M. May, *Virus dynamics*, Oxford University Press, 2000.

10. A. G. Lim, P. K. Maini, HTLV-I infection: a dynamic struggle between viral persistence and host immunity, *J. Theor. Biol.*, **352** (2014), 92–108. https://doi.org/10.1016/j.jtbi.2014.02.022

11. X. Pan, Y. Chen, H. Shu, Rich dynamics in a delayed HTLV-I infection model: Stability switch, multiple stable cycles, and torus, *J. Math. Anal. Appl.*, **479** (2019), 2214–2235. https://doi.org/10.1016/j.jmaa.2019.07.051

12. L. Wang, Z. Liu, Y. Li, D. Xu, Complete dynamical analysis for a nonlinear HTLV-I infection model with distributed delay, CTL response and immune impairment, *Discrete Contin. Dyn. Syst.*, **25** (2020), 917–933. https://doi.org/10.3934/dcdsb.2019196

13. S. Bera, S. Khajanchi, T. K. Roy, Dynamics of an HTLV-I infection model with delayed CTLs immune response, *Appl. Math. Comput.*, **430** (2022), 127206. https://doi.org/10.1016/j.amc.2022.127206

14. Y. Wang, J. Liu, J. M. Heffernan, Viral dynamics of an HTLV-I infection model with intracellular delay and CTL immune response delay, *J. Math. Anal. Appl.*, **459** (2018), 506–527. https://doi.org/10.1016/j.jmaa.2017.10.027

15. F. Li, W. Ma, Dynamics analysis of an HTLV-1 infection model with mitotic division of actively infected cells and delayed CTL immune response, *Math. Methods Appl. Sci.*, **41** (2018), 3000–3017. https://doi.org/10.1002/mma.4797

16. S. Li, Y. Zhou, Backward bifurcation of an HTLV-I model with immune response, *Discrete Contin. Dyn. Syst. B*, **21** (2016), 863–881. https://doi.org/10.3934/dcdsb.2016.21.863

17. S. Khajanchi, S. Bera, T. K. Roy, Mathematical analysis of the global dynamics of a HTLV-I infection model, considering the role of cytotoxic T-lymphocytes, *Math. Comput. Simul.*, **180** (2021), 354–378. https://doi.org/10.1016/j.matcom.2020.09.009

18. S. Chen, Z. Liu, L. Wang, X. Zhang, Global dynamics analysis for a nonlinear HTLV-I model with logistic proliferation and CTL response, *Int. J. Biomath.*, **17** (2024), 2350023. https://doi.org/10.1142/S1793524523500237

19. S. Chen, Z. Liu, L. Wang, X. Zhang, Stability and Hopf bifurcation analysis of a HTLV-I infection model with time-delay CTL immune response, *Discrete Contin. Dyn. Syst. B*, **29** (2024), 812–832. https://doi.org/10.3934/dcdsb.2023115

20. S. Chen, Z. Liu, X. Zhang, L. Wang, Dynamics and optimal therapy of a stochastic HTLV-1 model incorporating Ornstein-Uhlenbeck process, *Math. Methods Appl. Sci.*, **47** (2024), 9874–9896. https://doi.org/10.1002/mma.10099

21. W. Wang, W. Ma, Global dynamics of a reaction and diffusion model for an HTLV-I infection with mitotic division of actively infected cells, *J. Appl. Anal. Comput.*, **7** (2017), 899–930. https://doi.org/10.11948/2017057

22. A. M. Elaiw, N. H. AlShamrani, Analysis of a within-host HIV/HTLV-I co-infection model with immunity, *Virus Res.*, **295** (2021), 198204. https://doi.org/10.1016/j.virusres.2020.198204

23. A. M. Elaiw, N. H. AlShamrani, A. D. Hobiny, Mathematical modeling of HIV/HTLV co-infection with CTL-mediated immunity, *AIMS Math.*, **6** (2021), 1634–1676. https://doi.org/10.3934/math.2021098

24. S. Chowdhury, J. K. Ghosh, U. Ghosh, Co-infection dynamics between HIV-HTLV-I disease with the effects of cytotoxic T-lymphocytes, saturated incidence rate and study of optimal control, *Math. Comput. Simul.*, **223** (2024), 195–218. https://doi.org/10.1016/j.matcom.2024.04.015

25. R. Shi, Y. Zhang, Dynamic analysis and optimal control of a fractional order HIV/HTLV co-infection model with HIV-specific CTL immune response, *AIMS Math.*, **9** (2024), 9455–9493. https://doi.org/10.3934/math.2024462

26. H. Yang, X. Li, W. Zhang, A stochastic HIV/HTLV-I co-infection model incorporating the aids-related cancer cells, *Discrete Contin. Dyn. Syst. B*, **29** (2024), 702–730. https://doi.org/10.3934/dcdsb.2023110

27. A. M. Elaiw, A. S. Shflot, A. D. Hobiny, Stability analysis of SARS-CoV-2/HTLV-I coinfection dynamics model, *AIMS Math.*, **8** (2023), 6136–6166. https://doi.org/10.3934/math.2023310

28. A. M. Elaiw, E. A. Almohaimeed, A. D. Hobiny, Modeling the co-infection of HTLV-2 and HIV-1 in vivo, *Electron. Res. Arch.*, **32** (2024), 6032–6071. https://doi.org/10.3934/era.2024280

29. A. S. Perelson, D. E. Kirschner, R. D. Boer, Dynamics of HIV infection of CD4$^+$ T cells, *Math. Biosci.*, **114** (1993), 81–125. https://doi.org/10.1016/0025-5564(93)90043-a

30. H. Mohri, S. Bonhoeffer, S. Monard, A. S. Perelson, D. D. Ho, Rapid turnover of T lymphocytes in SIV-infected rhesus macaques, *Science*, **279** (1998), 1223–1227. https://doi.org/10.1126/science.279.5354.1223

31. D. S. Callaway, A. S. Perelson, HIV-1 infection and low steady state viral loads, *Bull. Math. Biol.*, **64** (2002), 29–64. https://doi.org/10.1006/bulm.2001.0266

32. H. Gómez-Acevedoa, M. Y. Li, S. Jacobson, Multistability in a model for CTL response to HTLV-I infection and its implications to HAM/TSP development and prevention, *Bull. Math. Biol.*, **72** (2010), 681–696. https://doi.org/10.1007/s11538-009-9465-z

33. P. Ngina, R. W. Mbogo, L. S. Luboobi, HIV drug resistance: insights from mathematical modelling, *Appl. Math. Model.*, **75** (2019), 141–161. https://doi.org/10.1016/j.apm.2019.04.040

34. B. E. Boukari, N. Yousfi, A delay differential equation model of HIV infection, with therapy and CTL response, *Bull. Math. Sci. Appl.*, **9** (2014), 53–68. https://doi.org/10.18052/www.scipress.com/BMSA.9.53

35. X. Song, Y. Li, Global stability and periodic solution of a model for HTLV-I infection and ATL progression, *Appl. Math. Comput.*, **180** (2006) 401–410. https://doi.org/10.1016/j.amc.2005.12.022

36. X. Jia, R. Xu, Global dynamics of a delayed HTLV-I infection model with Beddington-DeAngelis incidence and immune impairment, *Chaos Solitons Fract.*, **155** (2022), 111733. https://doi.org/10.1016/j.chaos.2021.111733

37. Y. Muroya, Y. Enatsu, H. Li, Global stability of a delayed HTLV-I infection model with a class of nonlinear incidence rates and CTLs immune response, *Appl. Math. Comput.*, **219** (2013), 10559–10573. https://doi.org/10.1016/j.amc.2013.03.081

38. L. Cai, X. Li, M. Ghosh, Global dynamics of a mathematical model for HTLV-I infection of CD4$^+$ T-cells, *Appl. Math. Model.*, **35** (2011), 3587–3595. https://doi.org/10.1016/j.apm.2011.01.033

39. K. Qi, D. Jiang, Threshold behavior in a stochastic HTLV-I infection model with CTL immune response and regime switching, *Math. Methods Appl. Sci.*, **41** (2018), 6866–6882. https://doi.org/10.1002/mma.5198

40. H. Gomez-Acevedo, M. Li, Global dynamics of a mathematical model for HTLV-I infection of T cells, *Can. Appl. Math. Q.*, **10** (2002), 71–86.

41. A. M. Elaiw, A. S. Shflot, A. D. Hobiny, Global stability of a general HTLV-I infection model with cytotoxic T-lymphocyte immune response and mitotic transmission, *Alex. Eng. J.*, **67** (2023), 77–91. https://doi.org/10.1016/j.aej.2022.08.021

42. H. L. Smith, P. Waltman, *The theory of the chemostat: dynamics of microbial competition*, Cambridge University Press, 1995. https://doi.org/10.1017/cbo9780511530043.003

43. A. Korobeinikov, Global properties of basic virus dynamics models, *Bull. Math. Biol.*, **66** (2004), 879–883. https://doi.org/10.1016/j.bulm.2004.02.001

44. J. K. Hale, S. M. V. Lunel, *Introduction to functional differential equations*, Springer-Verlag, 1993. https://doi.org/10.1007/978-1-4612-4342-7

45. H. K. Khalil, *Nonlinear systems*, 3 Eds., Prentice Hall, 2002.

46. J. Danane, K. Allali, Z. Hammouch, Mathematical analysis of a fractional differential model of HBV infection with antibody immune response, *Chaos Solitons Fract.*, **136** (2020), 109787. https://doi.org/10.1016/j.chaos.2020.109787

47. M. Awadalla, J. Alahmadi, K. R. Cheneke, S. Qureshi, Fractional optimal control model and bifurcation analysis of human syncytial respiratory virus transmission dynamics, *Fractal Fract.*, **8** (2024), 44. https://doi.org/10.3390/fractalfract8010044

48. Y. Guo, T. Li, Fractional-order modeling and optimal control of a new online game addiction model based on real data, *Commun. Nonlinear Sci. Numer. Simul.*, **121** (2023), 107221. https://doi.org/10.1016/j.cnsns.2023.107221

49. Z. Yaagoub, M. Sadki, K. Allali, A generalized fractional hepatitis B virus infection modelwith both cell-to-cell and virus-to-cell transmissions, *Nonlinear Dyn.*, **112** (2024), 16559–16585. https://doi.org/10.21203/rs.3.rs-3958680/v1

50. M. Renardy, C. Hult, S. Evans, J. J. Linderman, D. E. Kirschner, Global sensitivity analysis of biological multiscale models, *Curr. Opin. Biomed. Eng.*, **11** (2019), 109–116. https://doi.org/10.1016/j.cobme.2019.09.012

51. Z. Zi, Sensitivity analysis approaches applied to systems biology models, *IET Syst. Biol.*, **5** (2011), 336–346. https://doi.org/10.1049/iet-syb.2011.0015

52. A. Bazarbachi, Y. Plumelle, J. C. Ramos, P. Tortevoye, Z. Otrock, G. Taylor, et al., Meta-analysis on the use of zidovudine and interferon-alfa in adult T-cell leukemia/lymphoma showing improved survival in the leukemic subtypes, *J. Clin. Oncol.*, **28** (2010), 4177–4183. https://doi.org/10.1200/jco.2010.28.0669

53. A. O. Kamphorst, K. Araki, R. Ahmed, Beyond adjuvants: immunomodulation strategies to enhance T cell immunity, *Vaccine*, **33** (2015), B21–B28. https://doi.org/10.1016/j.vaccine.2014.12.082

54. C. H. Koh, S. Lee, M. Kwak, B. S. Kim, Y. Chung, CD8 T-cell subsets: heterogeneity, functions, and therapeutic potential, *Exp. Mol. Med.*, **55** (2023), 2287–2299. https://doi.org/10.1038/s12276-023-01105-x